Transportation Research Part C 158 (2024) 104450

Contents lists available at ScienceDirect

Transportation Research Part C

journal homepage: www elsevier com/locate/trc

Strategic driver repositioning in ride-hailing networks with dual sourcing

Tingting Dong [a], Qi Luo [b], Zhengtian Xu [c,*], Yafeng Yin [d], Jian Wang [e]

[a] Department of Civil and Environmental Engineering, The Hong Kong University of Science and Technology, Clear Water Bay, Kowloon, 999077, Hong Kong, China
[b] Department of Industrial Engineering, Clemson University, 277B Freeman Hall, Clemson, SC, 29634, United States
[c] Department of Civil and Environmental Engineering, The George Washington University, 800 22nd Street NW, Washington, DC, 20052, United States
[d] Department of Civil and Environmental Engineering, University of Michigan, 2350 Hayward Street, Ann Arbor, MI, 48109, United States
[e] Department of Transportation Engineering, Harbin Institute of Technology, 73 Huanghe Road, Harbin, Heilongjiang, 150001, China

ARTICLE INFO

Dataset link: https://gwu.box.com/s/1vw7jsay9ufwphv60n47pk4cun26myfu

Keywords:
Ride-hailing market
Dual sourcing
Network equilibrium
Supply management

ABSTRACT

In ride-hailing markets, the spatial mismatch between supply and demand characterizes one of the most fundamental operational bottlenecks. The voluntary customer search of drivers is oftentimes inadequate for narrowing the demand-supply gaps and falls short in responding timely to the dynamic market conditions. To facilitate better supply management, some ride-hailing platforms now adopt a dual-sourcing strategy by converting some freelance drivers as contractors, who would then follow platforms' guidance on repositioning movements when idle. This paper thus aims to analyze the implications of such a dual-sourcing strategy on the overall operations of ride-hailing services. We consider a monopolistic platform that owns a blended workforce, with freelance drivers searching for customers following their own preferences whilst contracted drivers repositioning in a centralized manner as system actuators. A mixed network equilibrium model is devised to capture the interplay between the idle repositioning movements of both parties. The theoretical existence of the mixed equilibrium is proved, and real-world data is invited to quantify the effects of dual sourcing on various market sectors. Our numerical results confirm the effectiveness of dual sourcing in smoothing operations, increasing customer demand, and driving up the revenue of ride-hailing services. However, the benefit of dual sourcing to the platform remains sensitive to the proportion of contractors in the entire workforce as well as the stimulative commission beyond their regular service income.

1. Introduction

Transportation Network Companies (TNCs) such as Uber and DiDi Chuxing act as intermediate platforms that swiftly connect ride-hailing customers with nearby drivers through digital applications (Wang and Yang, 2019). Accordingly, the service quality provided by the platform is heavily influenced by customer demand for rides and the availability of drivers within the spatial market. The spatial imbalance between supply and demand has a substantial impact on the operations of ride-hailing services, as demonstrated by empirical analysis using TNC data (Chen et al., 2015). This phenomenon arises partly because drivers tend to cluster in specific areas while becoming scarce in others. However, managing supply across spatial networks poses operational challenges. On the one hand, while it is essential to reposition drivers to meet future demand, achieving this is highly implausible given that

* Corresponding author.
E-mail address: zhengtian@gwu.edu (Z. Xu).

https://doi.org/10.1016/j.trc.2023.104450
Received 13 November 2023; Accepted 28 November 2023
Available online 19 December 2023
0968-090X/

the primary workforce of existing ride-hailing services consists of freelancers who have the freedom to select their preferred work schedules and service areas. On the other hand, freelancers can search strategically for potential customers to maximize their own profits, but they lack complete knowledge of market conditions, such as the demand distribution and the locations of other drivers. These factors cause significant frictions in matching supply and demand efficiently (Zha et al., 2018b).

TNCs typically employ pricing strategies to incentivize freelancers to relocate and counteract the spatiotemporal supply–demand mismatch (Bimpikis et al., 2019; Wang and Yang, 2019). For example, surge pricing enables the platform to dynamically raise prices in specific areas and periods (Cachon et al., 2017; Ma et al., 2020; Garg and Nazerzadeh, 2021; Hall et al., 2015; Besbes et al., 2021). The hypothesized mechanism is that freelancers who enjoy high flexibility will react to price surges and adjust their customer-searching movements and working schedules accordingly. Using an equilibrium analysis, Bimpikis et al. (2019) explored the theoretical potential of origin-based pricing for a platform's profitability. Lu et al. (2018) and Guda and Subramanian (2019) also investigated the merits of region-based pricing in mitigating the supply–demand imbalance and stimulating drivers toward hot-spot areas. While promising theoretical potentials are established on pricing, there is some pushback from the practice that questions the implementation and the equality issues related to spatial pricing. First, surge pricing can cause systematic earning disparities on drivers, even for those at the same origin, and thus discourage them from serving certain non-surging regions (Zuniga-Garcia et al., 2020). Meanwhile, whether the spatial surge pricing benefits customers also remains controversial (Zha et al., 2018b). Second, the setup of price surges can be challenging, and self-interested drivers can exploit tactless pricing mechanisms (Tripathy et al., 2022).

Demand rationing is considered as another efficient strategy for balancing spatial demand and supply (Afeche et al., 2023; Xu et al., 2020). It enables platforms to strategically decline ride requests in certain cases without price surges. Nevertheless, while a demand rationing strategy such as matching discrimination can free up supply resources and improve service efficiency, it raises concerns regarding the unequal treatment of riders, which harms the branding that TNCs strive to maintain. In addition, pricing and rationing strategies remain dependent on freelancers voluntarily seeking customers, which may still result in systemic demand-supply imbalances.

To address this issue at its core, one straightforward solution is to directly modify the composition of the workforce by reducing reliance on self-interested freelancers. Recently, some TNCs have expanded their single-sourcing supply of freelancers as dual sources by hiring dedicated contracted drivers (contractors), who submissively follow the platforms' scheduling and repositioning instructions. Being endowed with more managerial authority, the platform can accommodate the flexibility of freelancers with the predictability of contractors to improve the system's productivity. As two pioneering works on this topic, Dong and Ibrahim (2020) and Dong et al. (2021) applied aggregate models to explain why a dual-sourcing strategy can mitigate the labor shortage due to demand variation. However, their models, without a spatial structure, cannot inform how the introduction of contractors affects operational decisions such as idle drivers' repositioning. This study bridges this gap by characterizing the market equilibrium over a spatial network and examining strategies for repositioning contractors in a dual-sourcing environment. Specifically, freelancers reposition with their heterogeneous self-interested behaviors, whilst contractors as market actuators follow centralized guidance to mitigate the demand-supply imbalances. A monopolistic platform, in a role of a Cournot-Nash player, maximizes its overall revenue by whistling the contractors' repositioning. One challenge for modeling such a dual-sourcing market is to capture the interaction between centralized contractors' and self-interested freelancers' movements over the network. This paper develops a mixed network equilibrium (MNE) model with the objective of (a) characterizing the interplay between the dual-sourcing supply and the spatial customer demand; (b) investigating the platform's optimal repositioning policies for contractors; and (c) examining empirically the impact of dual sourcing on the status-quo ride-hailing market, especially its effectiveness in redistributing the supply to better match demand over the network.

The remainder of the paper is organized as follows. Section 2 begins with a comprehensive literature review, focusing on existing studies related to driver repositioning and dual sourcing in ride-hailing markets, and highlights the unique perspectives taken in this study. Section 3 formulates drivers' spatial repositioning under two special cases with freelancers and contractors serving as the sole source of labor in ride-hailing services, respectively. The repositioning models outlined in both cases set the stage for the MNE model with dual sourcing, which is then formally presented in Section 4. An iterative solution algorithm for solving the optimal repositioning strategies is developed in Section 5, while Section 6 details the empirical data and contextual setups for numerical experiments. Section 7 then conducts numerical analysis with various performance metrics retrieved for drivers, customers, and the platform, to comprehensively evaluate the impacts of dual sourcing. In addition, Section 8 investigates the matching differentiation between freelancers and contractors in the MNE and glimpses the multifaceted consequences on the system performance. The paper concludes with the main findings and future research avenues in Section 9.

2. Literature review

The mixed equilibrium under dual sourcing represents an intermediate product, with freelancers and contractors respectively following decentralized (Yang and Wong, 1998; Buchholz, 2022; Bimpikis et al., 2019) and centralized (Iglesias et al., 2019; Braverman et al., 2019; Banerjee et al., 2017) customer-searching disciplines but forming interdependence in between.

In the decentralized discipline, extensive studies analyzed drivers' self-interested customer searching behavior and incorporated their strategic decisions into network equilibrium models. Yang and Wong (1998) made the first attempt to develop a static network equilibrium model that describes taxi movements for given customer demand. Each idle driver chooses her target zones to minimize the expected searching time for the next customer, whose zonal choices are described by a logit model. Such a framework has been extended to account for elastic demand and congestion (Wong et al., 2001; Xu et al., 2021a), bilateral searching (Yang et al., 2010b), and e-haling services (He et al., 2018). To account for temporal market fluctuations, Buchholz (2022) constructed a dynamic

equilibrium model in which drivers' utility and repositioning decisions are time-dependent. Zhang et al. (2023) adopted a game-theoretical approach and described drivers' dynamic routing problems as Markov decision processes. These works are built upon their spatial network equilibrium models that characterize the ride-hailing market at (time-dependent) steady states. Recently, Beojone and Geroliminis (2023) investigated individualized relocation guidance within an extensive context of co-existing ride-hailing and ride-splitting services to tailor strategies that maximize drivers' expected earnings.

For the centralized operations, research studies have been devoted to the optimization and solution of empty vehicles' repositioning for various managerial objectives (Özkan and Ward, 2020; Liu and Samaranayake, 2020; Lei et al., 2020; Li et al., 2021; Yang and Ramezani, 2022). For example, Guo et al. (2021) integrated platforms' matching strategies with vehicles' repositioning decisions to hedge the uncertain market demand. Braverman et al. (2019) examined the empty vehicle repositioning problem using a closed queueing network model and proved that the fluid-based approach can provide asymptotically optimal routing strategies in a finite-vehicle setting. Besides, Wen et al. (2017) and Jiao et al. (2021) developed practical frameworks based on the deep reinforcement learning method and conducted real-world experiments to verify its effectiveness. Yang and Ramezani (2022) later proposed a learning method that outputs real-time multi-vehicle repositioning policy by accounting for the platform's long-term efficiency. A comprehensive survey can be found at Wang and Yang (2019) and Zardini et al. (2022). In general, this research stream assumes that idle drivers fully adhere to the repositioning guidance provided by the platform. This assumption aligns more effectively with scenarios where compliant contractors represent the primary labor source. Building upon the framework established by these studies, we formulate contractors' centralized repositioning as an optimization problem. Nonetheless, existing research often considers vehicle repositioning alongside other operational decisions (Zardini et al., 2022; Narayanan et al., 2020), whereas our focus lies on the former.

Despite extensive research conducted on both decentralized and centralized repositioning of drivers, the investigation on the intermediate level is rather limited. The consideration of dual sources further complicates the interaction between market supply and demand. The repositioning decisions for centralized contractors influence trip demand both directly and indirectly, through their effects on the availability of drivers and the movement of self-interested freelancers. The key challenge lies in capturing such intricate interactions over a spatial network in a unifying model framework.

As a related variant of dual labor sources, recent studies have developed equilibrium models in the mixed-autonomy contexts, where both autonomous and human-driven vehicles coexist to offer services (Wei et al., 2019, 2020; Yang et al., 2020). Wei et al. (2019) considered the context where autonomous vehicles get matched after the depletion of human-driven vehicles, and discovered that a mixed-autonomy fleet does not always outperform that of human-driven vehicles alone. They then extended the work to other priority matching schemes performed uniformly over the network (Wei et al., 2020). These early efforts on mixed autonomy assumed perfect matching between customers and drivers. Customers either get matched and picked up immediately or they exit the market. Thus, customers' trip demand is independent of service quality characterized by service delay. However, customers' delay sensitivity is a distinct feature for on-demand services, where platforms strive to improve service quality by lessening customers' waiting time (Taylor, 2018). Besides, the relative spatial distance is an important factor in drivers' repositioning decisions. Despite the resultant beauty of math, the omission of these aspects of considerations yields troubles when applying the models for practical repositioning decision-making. The proposed model addresses these gaps by explicitly accounting for the endogeneity between service demand and quality as well as incorporating repositioning distance into the decisions of both drivers and platforms.

The contribution of our study is threefold. First, we introduce a mixed network equilibrium model that captures the complexity arising from the heterogeneity and interactions of repositioning movements between freelanced and contracted drivers. Second, a theoretical proof for the existence of market equilibrium is provided within the proposed framework, and an effective algorithm is devised for solving the equilibrium solutions. Third, we conduct an extensive case study using real-world ride-hailing trip data, allowing us to derive valuable insights regarding the implications of dual-sourcing strategies on various stakeholders.

3. Network equilibrium with single sourcing

Consider a spatial network $\mathcal{N}(V\ A)$, where V is the set of vertices consisting of customers' origin zones I and destination zones J, i.e., $V = I \cup J$, and A is the set of arcs connecting in between. Each trip request leads from one origin zone to a destination zone, and drivers circulate over the space to provide non-pooling ride services. The trip-wise travel time, fare, and driver commission are assumed to be fixed and exogenous in this paper. A platform then matches trip requests to idle drivers within the origin zone and collects the revenue on trip completion. In the given context, this section introduces two network equilibrium models that correspond to the single-sourcing scenarios. One model focuses on self-interested freelancers, while the other model addresses obedient contractors with centralized repositioning decisions. Notations in this paper are summarized in Appendix A for readers' reference.

3.1. Network equilibrium with freelance drivers

The network equilibrium with only freelancers is similar to those of the conventional taxi or ride-hailing markets (Yang et al., 2010a; Xu et al., 2021a). The following collects the major components to assemble the base model.

3.1.1. Modeling components

Demand of ride-hailing market. Denote W as the set of origin and destination (OD) pairs, i.e., $W = \{(i\ j)|i \in I\ \ j \in J\}$. For each given hour and each OD pair, the demand for trip services Q_{ij} (trips/hr) is assumed to be a decreasing continuous function of the waiting time w_i^p (or service delay) that customers experience at origin zone i:

$$Q_{ij} = Q_{ij}^0 \quad f\left(w_i^p | F_{ij}\ \ h_{ij}\right) \qquad \forall (i\ \ j) \in W \tag{1}$$

where Q_{ij}^0 denotes the potential demand from zone i to j; the parameters F_{ij} and h_{ij} represent the exogenous trip fare and in-vehicle service duration; and the superscript p labels passengers. Under the single-sourcing context, the number of trips served by freelancers Q_{ij}^f equalizes the realized demand Q_{ij} for each OD pair $(i\ \ j) \in W$.

Self-interested repositioning of freelancers. After dropping off customers at their destination zones, freelance drivers decide target origin zones to search for the next customers. Denote T_{ji}^{vf} as the idle freelancer flow from zone j to zone i. The associated utility U_{ji} subtracts the operating cost from the average trip earnings of drivers:

$$U_{ji} = \hat{E}_i - \gamma_1 \quad (h_{ji} + \hat{h}_i) - \gamma_2 \quad w_i^{vf} \qquad \forall j \in J\ \ i \in I$$

where $\hat{E}_i$ and $\hat{h}_i$ are drivers' perceived earning and delivery time of trips that originate from zone i; the travel time h_{ji} from zone j to i is the sunk cost drivers spend repositioning; the waiting time w_i^{vf} is the average time that drivers spend being idle at zone i before matching with a customer, which is an endogenous variable; parameter γ_1 and γ_2 denote drivers' value per unit travel time and per unit idle time, respectively. Collectively, the composite component $\gamma_1 \quad (h_{ji} + \hat{h}_i) + \gamma_2 \quad w_i^{vf}$ represents a driver's total expected time cost across the stages of dropping off a customer in zone j, repositioning to zone i, picking up a new customer therein and delivering her. Specifically, the perceived earning $\hat{E}_i$ and delivery time $\hat{h}_i$ are subject to drivers' risk attitudes and behaviors, which are described by the following functions:

$$\hat{E}_i = G_e\left(\{E_{id}\ \ Q_{id}\}_{d:(i\ d) \in W}\right) \qquad \hat{h}_i = G_h\left(\{h_{id}\ \ Q_{id}\}_{d:(i\ d) \in W}\right) \qquad \forall i \in I \tag{2}$$

where E_{id} is a driver's earning per completed trip from zone i to d for all $(i\ \ d) \in W$. Without loss of generality, we assume that both mappings $G_e(\ )$ and $G_h(\ )$ are continuous with respect to their inputs, and the outputs are bounded by the values of $\{E_{id}\}$ and $\{h_{id}\}$, respectively, i.e., $\hat{E}_i \in [\min_{(i\ d) \in W} E_{id}\ \ \max_{(i\ d) \in W} E_{id}]$ and $\hat{h}_i \in [\min_{(i\ d) \in W} h_{id}\ \ \max_{(i\ d) \in W} h_{id}]$.

Freelance drivers make repositioning decisions to maximize their own utility. However, due to the imprecision in market observations and the stochastic nature in market realizations, drivers' perceived utility may contain errors. To account for this, we introduce a random error term ϵ^0 to represent the noise in freelancers' perceived utility for each zonal choice. Specifically, a freelancer in zone j will choose to search for customers in zone i if $U_{ji} + \epsilon_i^0 \geq U_{jm} + \epsilon_m^0$ for any $m \in I$. We further assume freelancers' perception errors follow an independently and identically-distributed Gumbel distribution, which has been extensively used and empirically validated in taxi markets (Wong et al., 1999). With these prescriptions, the probability $Pr_{i/j}$ that an idle freelancer in zone j would search customers in zone i is given by a logit function:

$$Pr_{i/j} = \frac{\exp(\theta U_{ji})}{\sum_{m \in I} \exp(\theta U_{jm})} \qquad \forall i \in I\ \ j \in J \tag{3}$$

where θ is a non-negative parameter and measures the degree of dispersion on drivers' perception error. Drivers make random selections of repositioning destinations when θ approaches 0, but target uniformly toward the zone with the highest true utility U_{ji} when θ approaches $+\infty$. As a result, the flow of idle drivers T_{ji}^{vf} is given by:

$$T_{ji}^{vf} = \sum_{m:(m\ j) \in W} Q_{mj}^f \quad Pr_{i/j} \qquad \forall i \in I\ \ j \in J.$$

Besides, at the steady state, T_{ji}^{vf} satisfies the following flow balance constraints:

$$\sum_{j \in J} T_{ji}^{vf} = \sum_{j:(i\ j) \in W} Q_{ij}^f \qquad \forall i \in I \tag{4}$$

$$\sum_{i \in I} T_{ji}^{vf} = \sum_{i:(i\ j) \in W} Q_{ij}^f \qquad \forall j \in J. \tag{5}$$

These equalities ensure that the idle movements of drivers should match the flow of assigned trip requests at both origin and the destination zones.

Pickup time of drivers for customers. Customers' average waiting time endogenously depends on the density of idle drivers within each origin zone. Suppose the platform executes quick matching for customers such that all incoming requests are matching immediately to nearby drivers without matching delays. Then, customers' waiting time simply equals their pickup time after getting matched (Castillo et al., 2017). Denote N_i^{vf} as the number of idle drivers in zone i. Then, the pickup time of customers could be specified as follows:

$$w_i^p = f_w(N_i^{vf}) \qquad \forall i \in I.$$

where $f_w(\,)$ prescribes a non-negative decreasing function regarding its inputs. Without loss of generality, we assume that $f_w(\,)$ is twice differentiable and satisfies $f_w'' > 0$. i.e., increasing the number of idle drivers leads to a diminishing marginal return in reducing pickup times. By Little's law, at steady state, the number of idle freelancers N_i^{vf} at zone i satisfies:

$$N_i^{vf} = \sum_{j\in I} T_{ji}^{vf} \quad w_i^{vf} \qquad \forall i \in I.$$

Freelancers' fleet conservation. Denote N^f as the total number of freelancers in service. The fleet conservation condition is given as

$$N^f = \sum_{j\in J}\sum_{i\in I} T_{ji}^{vf} \quad (h_{ji} + w_i^{vf}) + \sum_{(i\ j)\in W} Q_{ij}^f \quad \left(w_i^p + h_{ij}\right)$$

where the right-hand-side terms expand the number of freelancers over the stages of spatial repositioning, idling for matching, picking up customers, and delivering them, respectively.

3.1.2. Network equilibrium model

Assembling all the above relationships yields a network equilibrium model (6) that solves freelancers' idle movements $\{T_{ji}^{vf}\}$ in a single-sourcing ride-hailing market:

$$Q_{ij}^f = Q_{ij}^0 \quad f\left(w_i^p | F_{ij}\ \ h_{ij}\right) \qquad \forall (i\ \ j) \in W \tag{6a}$$

$$T_{ji}^{vf} = \left(\sum_{m:(m\ j)\in W} Q_{mj}^f\right) \frac{\exp(\theta U_{ji})}{\sum_{m\in I}\exp(\theta U_{jm})} \qquad \forall j \in J\ \ i \in I \tag{6b}$$

$$U_{ji} = G_e(\{E_{id}\ \ Q_{id}^f\}_{d:(i\ d)\in W}) - \gamma_1 \quad \left(h_{ji} + G_h(\{h_{id}\ \ Q_{id}^f\}_{d:(i\ d)\in W})\right) - \gamma_2 \quad w_i^{vf} \qquad \forall j \in J\ \ i \in I \tag{6c}$$

$$\sum_{j\in J} T_{ji}^{vf} = \sum_{j:(i\ j)\in W} Q_{ij}^f \qquad \forall i \in I \tag{6d}$$

$$w_i^p = f_w(N_i^{vf}) \qquad \forall i \in I \tag{6e}$$

$$N_i^{vf} = \sum_{j\in J} T_{ji}^{vf} \quad w_i^{vf} \qquad \forall i \in I \tag{6f}$$

$$N^f = \sum_{j\in J}\sum_{i\in I} T_{ji}^{vf} \quad h_{ji} + \sum_{i\in I} N_i^{vf} + \sum_{(i\ j)\in W} Q_{ij}^f \quad \left(w_i^p + h_{ij}\right). \tag{6g}$$

Specifically, $z^f = \{Q_{ij}^f\ \ w_i^p\ \ T_{ji}^{vf}\ \ U_{ji}\ \ w_i^{vf}\ \ N_i^{vf}\}$ is the collection of endogenous variables to be solved for market equilibrium when freelance drivers serve as the sole labor source. Under mild conditions, the existence of such a market equilibrium has been proved (Xu et al., 2021a).

3.2. Centralized repositioning policy with contracted drivers

When compliant contractors serve as the single labor source, the number of trips taken by contractors Q_{ij}^c equals the total realized demand Q_{ij} for each OD pair $(i\ \ j) \in W$ and customers' pickup time w_i^p is uniquely dependent on the number of idle contractors N_i^{vc} in each zone $i \in I$. Because contractors adhere to the centralized routing instructions, the centralized repositioning model disregards individual strategic repositioning behaviors.

We assume the platform guides the movements of idle contractors to maximize the system revenue. Contractors received a fixed salary as permanent employees, which is an exogenous parameter in the centralized model. Let N^c denote the number of active contractors, T_{ji}^{vc} be contractors' repositioning flow from destination zone j to origin zone i, and w_i^{vc} be their average waiting time before getting matched with customers in zone i. The centralized repositioning policy for contractors $\{T_{ij}^{vc}\}$ solves the following optimization problem:

$$\max_{z_0^c \ge 0} \pi(Q_{ij}^c) = \sum_{(i\ j)\in W} F_{ij} \quad Q_{ij}^c \tag{7a}$$

$$\text{s.t.} \quad Q_{ij}^c = Q_{ij}^0 \quad f\left(w_i^p | F_{ij}\ \ h_{ij}\right) \qquad \forall (i\ \ j) \in W \tag{7b}$$

$$w_i^p = f_w(N_i^{vc}) \qquad \forall i \in I \tag{7c}$$

$$N_i^{vc} = \sum_{j\in J} T_{ji}^{vc} \quad w_i^{vc} \qquad \forall i \in I \tag{7d}$$

$$\sum_{j\in J} T_{ji}^{vc} = \sum_{j:(i\ j)\in W} Q_{ij}^c \qquad \forall i \in I \tag{7e}$$

$$\sum_{i\in I} T_{ji}^{vc} = \sum_{i:(i\ j)\in W} Q_{ij}^c \qquad \forall j \in J \tag{7f}$$

$$\sum_{(i\ j)\in W} Q_{ij}^c \quad \left(h_{ij} + w_i^p\right) + \sum_{j\in J}\sum_{i\in I} T_{ji}^{vc} \quad h_{ji} + \sum_{i\in I} N_i^{vc} = N^c \tag{7g}$$

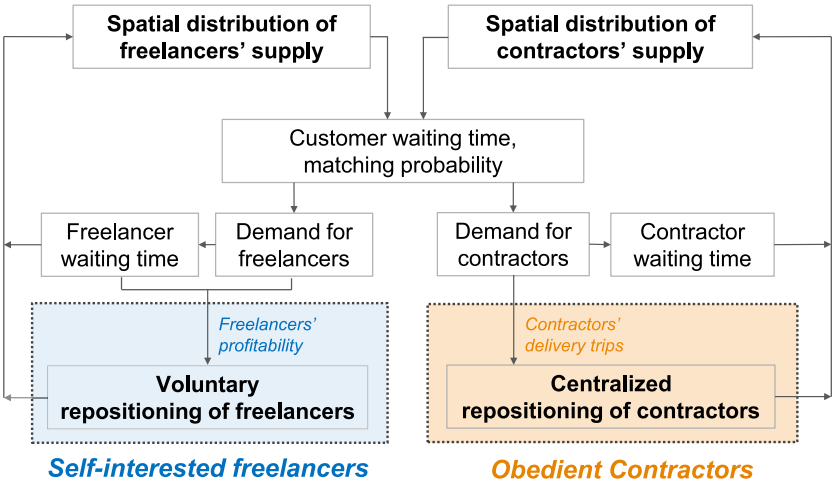

Fig. 1. Interaction between customers and drivers of the two labor sources.

where π specifies the system revenue, and $z_0^c = \{Q_{ij}^c \ N_i^{vc} \ w_i^p \ T_{ji}^{vc} \ w_i^{vc}\}$ is the collection of decision variables when contractors serve as single labor source. Constraints (7b)–(7g) confine contractors' idle and occupied movements related to the aggregate customer demand. Among them, constraint (7d) results from Little's law; (7e) and (7f) ensure the flow balances at the origins and destinations, respectively; and (7g) specifies the fleet conservation for contractors.

4. Mixed network equilibrium with dual sourcing

This section extends the network models to consider MNE with both freelancers and contractors. We first clarify the market setting for dual sourcing and detail the modeling components to delineate the strategic interactions between two labor sources. Then, the concept of mixed network equilibrium is formally introduced and the existence of equilibrium is proved. The end of this section discusses major model assumptions and outlines their relaxation.

4.1. Market setting

With dual sources, a mixed labor supply of N^f freelancers and N^c contractors circulate in the network to provide on-demand services. The spatial distribution of idle freelancers and contractors influences the market realizations characterized by trip demand and the waiting time of customers and drivers. Freelancers and the platform act as players who are presumed to make repositioning decisions given their knowledge of the other players. After observing market conditions, freelancers when idle would cruise to search for customers in zones with maximal perceived utility. Meanwhile, the monopolistic platform acts as a Cournot-Nash player who controls the contractors' repositioning movements to maximize its overall revenue. It makes repositioning decisions in responding to market conditions and the instantaneous spatial distribution of idle freelancers.[1] Fig. 1 summarizes the interaction between the two labor sources as well as the shared pool of customer demand in a ride-hailing market. The key challenge is to characterize the interplay among these market components and then bundle them as consistent mathematical correspondences over the network structure. The following rematerializes the modeling components for the dual-sourcing setting, devises their connections, and puts forward an MNE model to delineate the service state of a ride-hailing network.

4.2. Modeling components

Note that the repositioning decisions of the platform and strategic freelancers are interconnected by influencing the spatial distribution of idle drivers and market states. Therefore, to neutrally represent the market structure, here we introduce a dummy market operator in addition to the platform and freelancers. The dummy operator takes the platform's order-matching policy, based on the spatial distribution of idle freelancers and contractors, and executes market state values. This partitions the MNE model into three components that respectively delineate intrinsic system relationships, the platform's repositioning policy for contractors, and the strategic repositioning behaviors of freelancers.

[1] Here, we consider a Cournot-Nash game. However, as we model freelancers' responses by a system of equations, the model developed in this paper can be easily adapted to delineate Stackelberg games where the platform acts as a leader and freelancers are followers.

4.2.1. Intrinsic system relationships

Let k denote the driver type with $k \in \{f\ c\}$, and the superscripts f and c label terms corresponding to freelancers and contractors, respectively. We characterize the current market status by a tuple $\zeta = \left(\{Q_{ij}^k\}_{(i\ j)\in W}\ \{w_i^p\}_{i\in I}\ \{w_i^{vk}\}_{i\in I}\right)$, with Q_{ij}^k being the trip demand served by type-k drivers for each OD pair $(i\ j) \in W$ and w_i^{vk} being type-k drivers' average waiting time at zone i. Given the number of type-k idle drivers N_i^{vk} at each zone i, the market status ζ is uniquely determined, and is calculated by the following function:

$$\zeta = g(\boldsymbol{N}^{vc}\ \boldsymbol{N}^{vf}) \tag{8}$$

where vector $\boldsymbol{N}^{vk} = (N_i^{vk})_{i\in I}$ represents the spatial distribution of type-k idle drivers; and function $g(\ )$ assembles the calculating rules for updating ζ (Eqs. (10), (11), and (12)), which is explained below.

Demand of ride-hailing market. The customer demand function remains the same as the single-sourcing counterpart, see Eq. (1). But with contractors and freelancers coexisting to offer trip services, the realized demand now satisfies the following relationship,

$$Q_{ij} = Q_{ij}^c + Q_{ij}^f \quad \forall (i\ j) \in W. \tag{9}$$

where the number of trips served by two types of drivers Q_{ij}^c and Q_{ij}^f endogenously depend on the platform's matching policies.

Matching policy with dual sources. The matching policy could directly impact the trip demand served by each type of driver and hence their occupied and idle movements over the network. For simplicity, we assume that idle freelancers and contractors are scattered independently following the spatial Poisson Point Process, and the platform matches trip requests to the closest available driver nearby regardless of her service types. In other words, it is assumed that the platform does not differentiate freelancers and contractors in the matching process. A more general modeling treatment is discussed in Section 8 that discards such an assumption by permitting matching priority between the two types of drivers.

For each driver type $k \in \{f\ c\}$, let P_i^k denote the probability that a trip request originating at zone i is matched with a type-k driver. Then, without matching differentiation, the matching probabilities are

$$P_i^k = \frac{N_i^{vk}}{N_i^{vc} + N_i^{vf}} \quad \forall i \in I\ \ k \in \{f\ c\}.$$

Accordingly, the number of trips served by each type of driver satisfies

$$Q_{ij}^k = Q_{ij}^0\ \ f\left(w_i^p | F_{ij}\ h_{ij}\right)\ \ \frac{N_i^{vk}}{N_i^{vf} + N_i^{vc}} \quad \forall (i\ j) \in W\ \ k \in \{f\ c\}. \tag{10}$$

Waiting time of customers. Freelancers and contractors are treated identically in the matching process and thus experience the same amount of time on average for picking up customers after getting matched. The average pickup time w_i^p decreases with the density of idle contractors and freelancers and now formulates

$$w_i^p = f_w(N_i^{vc} + N_i^{vf}) \quad \forall i \in I \tag{11}$$

where the inputs of function $f_w(\ )$ contains the idle drivers from both service types.

Waiting time of drivers. Without order-matching differentiation, freelancers and contractors are expected to experience the same amount of idle waiting time before getting matched with a customer at each origin zone. Following Little's law on idle driver supply (Eqs. (6f) and (7d)) and the flow balance conditions for each driver type (Eqs. (6d) and (7e)), drivers' average waiting time w_i^{vk} can also be expressed as follows,

$$w_i^{vk} = \frac{\sum_{k\in\{f\ c\}} N_i^{vk}}{\sum_{k\in\{f\ c\}} \sum_{j:(i\ j)\in W} Q_{ij}^k} \quad \forall i \in I\ \ k \in \{f\ c\}. \tag{12}$$

4.2.2. Platform's repositioning policy for contractors

The platform observes the spatial distribution of idle drivers $\boldsymbol{N}^{vk}$ and the current market status ζ characterized by the trip demand served by two labor sources $\{Q_{ij}^k\}$, current customers' average waiting time $\{w_i^p\}$, and drivers' average waiting time $\{w_i^{vk}\}$. With such knowledge, the platform plays the role of a Cournot-Nash player and calls the repositioning of contractors to maximize the overall expected system revenue π. Given fixed trip fare F_{ij}, the revenue π is determined by the expected realized demand Q_{ij}, which routes back to the availability of contractors in each zone and their flow across zones. Given its knowledge of market status ζ and the distribution of idle freelancers N_i^{vf}, the platform's repositioning decisions for contractors $\{T_{ji}^{vc}\}$ solve the following problem:

$$\max_{z^c\geq 0} \pi(\boldsymbol{N}^{vc}|\zeta\ \boldsymbol{N}^{vf}) = \sum_{(i\ j)\in W} F_{ij}\ \ Q_{ij}^0\ \ f\left(f_w(N_i^{vc} + N_i^{vf})\right) \tag{13a}$$

s.t. (7d), (7e), (7f), (7g)

where $z^c = \{N_i^{vc}\ T_{ji}^{vc}\}$ is the collection of decision variables. The above problem is similar to the single sourcing optimization problem (7), but with different specifications regarding market demand and with ζ serving as input parameters. For brevity, the

feasible region of decision variables z^c prescribed by (7d)–(7g) along with the non-negativity constraints is denoted as $\Omega^c(\zeta\ \boldsymbol{N}^{vf})$, i.e.,

$$\Omega^c(\zeta\ \boldsymbol{N}^{vf}) = \{z^c | (7d)\text{–}(7g)\quad z^c \geq 0\}.$$

4.2.3. Freelancers' repositioning decisions

After observing current market status ζ, an individual idle freelancer chooses a zone that maximizes her perceived utility as in the pure-freelancer case. Given ζ, freelancers' utility can be calculated by Eq. (6c) and their idle flow pattern $\{T_{ji}^{vf}\}$ could still be described by the logit function (6b). For each origin zone, the resultant expected spatial distribution of idle freelancers $\boldsymbol{N}^{vf}$ satisfies Eq. (6f). We denote $z^f = \{T_{ji}^{vf}\ N_i^{vf}\ U_{ji}\}$ as the collection of freelancers' decisions thereafter. For brevity, given ζ, the variables z^f prescribed by Eqs. (6b), (6c), and (6f) is denoted as $\Omega^f(\zeta)$, i.e.,

$$\Omega^f(\zeta) = \{z^f | (6b), (6c), (6f)\}.$$

4.3. Formulation and existence of MNE

The MNE is materialized in accordance with the principle that the platform and individual freelancers both make the best responses in their repositioning decisions given their perception of the market condition. At equilibrium, the market reaches a steady state where the market conditions are self-sustaining and the movements of idle contractors and freelancers meet the trip demand at every origin zone. With the above specifications, the MNE integrates the following interdependent decision-making and steady-state conditions:

(a) The repositioning decision of the platform z^{c*} solves

$$z^{c*} = \underset{z^c \in \Omega^c(\zeta\ \boldsymbol{N}^{vf})}{\operatorname{argmax}}\ \pi(\boldsymbol{N}^{vc} | \zeta\ \boldsymbol{N}^{vf}) \quad \text{where } \boldsymbol{N}^{vf} \in z^f; \tag{14a}$$

(b) The repositioning decision of freelancers z^f solves

$$z^f \in \Omega^f(\zeta) \tag{14b}$$

(c) The market reaches an steady state when we have (6d), (6g), and the following (14c),

$$\zeta = g(\boldsymbol{N}^{vc}\ \boldsymbol{N}^{vf}) \quad \text{where } \boldsymbol{N}^{vc} \in z^{c*}\ \boldsymbol{N}^{vf} \in z^f; \tag{14c}$$

The calculation of MNE solves $(z^{c*}\ z^f)$ and ζ that are mutually reconcilable as inputs and outputs in (14). Since market status ζ depends on the decisions of both the platform and individual freelancers, solving z^{c*} and z^f essentially solves the best response of each player when the others' decisions are held constant. Such a structure resonates with that of the traffic assignment problem with mixed user behaviors. As initiated by Harker (1988), the traffic states were materialized as a network equilibrium between multiple Cournot-Nash players, each minimizes its own costs treating all other players' flows as fixed. Similarly, to extend our model for competitive market cases with multiple profit-maximizing platforms, each platform can be incorporated in parallel as an additional Cournot-Nash player that manages a group of contractors, while freelancers remain as Wardropian players. Conversely, by setting the fleet size of freelancers or contractors to zero, the above model structure reduces to single-sourcing models discussed in Section 3.

The aforementioned MNE model takes system states as an intermediary and captures drivers' strategic repositioning behaviors over a spatial network. Notice that the trip demand function $f(\,)$ and customers' pickup function $f_w(\,)$ influence the system realizations and platform's repositioning decisions, and hence the MNE solutions. To theoretically examine the equilibrium existence, we make the following specification on functions $f(\,)$ and $f_w(\,)$ as well as the network structure:

- C.1 Both $f(x)$ and waiting time function $f_w(x)$ are twice differentiable on x. Given $x > 0$, the value of derivatives $f'(f_w(x))$ has an upper limit.
- C.2 Given $x \geq 0$, waiting time function $f_w(x)$ is positively valued and upper bounded.
- C.3 Given $x \geq 0$, the composition of function $f(f_w(x))$ satisfies $f(f_w(x)) > 0$ and $\lim_{x\to 0} f(f_w(x)) = 0$. With this, we have the conditions $\lim_{N_i^{vc}+N_i^{vf}\to 0} Q_{ij} = 0$ and $\lim_{N_i^{vc}+N_i^{vf}\to 0} Q_{ij}^c = 0$ hold for any OD pair $(i\ j) \in W$.
- C.4 The composition of functions $f(f_w(x))$ is strictly concave over the domain $x \geq 0$.
- C.5 Given $x \in (0\ N^c + N^f)$, the value of $x/f(f_w(x))$ has an upper limit.
- C.6 The network $\mathcal{N}(V\ A)$ defines a strongly connected graph.

Recall that the trip demand Q_{ij} can be expressed as $Q_{ij} = Q_{ij}^0 f(f_w(N_i^{vc} + N_i^{vf}) | F_{ij}\ h_{ij})$ for each OD pair $(i\ j) \in W$ (see Eqs. (9), (10), and (11)), Condition C.1 implies that trip demand changes continuously with the supply of idle drivers at zone i and its rate of change has an upper limit. Condition C.2 suggests that customers have a tolerance for their waiting time. If their average waiting time exceeds the maximum waiting time, they will cancel the trip and turn to other alternative modes. Condition C.3 states that no trips would be served at an origin zone if there are no available idle drivers. Condition C.4 indicates that the marginal return of idle driver supply is diminishing, which is a commonly adopted assumption (Yang et al., 2010a; Zha et al., 2018a). Condition C.5 states that the average waiting time of drivers has an upper limit. Finally, Condition C.6 ensures that there exists a path connecting each pair of zones over the network $\mathcal{N}(V\ A)$.

With the above conditions, the existence of mixed network equilibrium is guaranteed, as we state in Theorem 1.

Theorem 1 (*Existence of Mixed Network Equilibrium*). *If conditions C.1–C.6 are satisfied, there exists at least one equilibrium solution to the MNE model defined by (14).*

Readers can refer to Appendix B.1 for the proof of Theorem 1 and the relevant lemmas and propositions. Note that the MNE solution is unlikely to be unique in view of the fact that multiple equilibria exist even in an isotropic market when pickup times are endogenous (Castillo et al., 2017). Readers could refer to Appendix B.3 for further discussions on the existence of multiple equilibria.

4.4. Discussion on model assumptions

The proposed model characterizes the market equilibrium under dual sourcing, which posits several technical assumptions. The following summarizes the major assumptions made in the analysis and outlines possible relaxations to approach:

1. The current model assumes that the total numbers of contractors N^c and freelancers N^f are exogenous variables. When drivers' reservation wage is taken into account (Dong et al., 2021), one can add an additional equation and easily incorporate the elastic supply into this framework.
2. We assume that freelancers' perception errors regarding their utility are independently and identically distributed Gumbel variables, which results in a logit choice function. The assumption of identical distribution can be relaxed by involving the weibit model (Castillo et al., 2008). Other alternative distribution functions could also be viable substitutes, though they could lead to choice functions that are not analytically tractable. As more data becomes available, we can calibrate and integrate more precise discrete choice models, as exemplified by Urata et al. (2021).
3. The travel time between zones is assumed to be constant, ignoring potential congestion effects caused by ride-hailing drivers' repositioning decisions. This is applicable in situations where ride-hailing services account for a small portion of overall traffic volumes while their interactions with regular traffic are negligible. When the congestion effects become pronounced, one can incorporate a flow-dependent travel time function as well as complementarity constraints to endogenize traffic dynamics (Xu et al., 2021a).

5. Solution algorithm

Given the exposed structure, this section interprets the MNE as a fixed-point problem and then develops an iterative procedure that is tractable with prevailing optimization solvers for efficient solutions.

5.1. MNE as a fixed-point problem

The composition of MNE model reveals a natural fixed-point problem structure that starts and loops back at the distribution of idle contractors and freelancers ($\boldsymbol{N}^{vc}$ $\boldsymbol{N}^{vf}$). Specifically, taking ($\boldsymbol{N}^{vc}$ $\boldsymbol{N}^{vf}$) as parametric inputs uniquely determines market status ζ through Eqs. (10), (11), and (12). With ζ and $\boldsymbol{N}^{vf}$, the platform's revenue maximization problem (13) is expected to solve z^c and hence the distribution of idle contractors $\boldsymbol{N}^{\boldsymbol{vc}}$. Meanwhile, for given ζ, applying Eqs. (6b), (6c), and (6f) is expected to lead to an updated distribution of idle freelancers $\boldsymbol{N}^{vf}$. However, directly applying such a fixed-point problem might fail to obtain an equilibrium solution because problem (13) could be infeasible, and the conditions (6d) and (6g) are not guaranteed to be satisfied by $\boldsymbol{N}^{vf}$. To avoid infeasibility during the iterative process, we introduce demand adjusters ϕ_i^k for each origin zone i and for each driver type $k \in \{f\ c\}$ that scales the trip demand Q_{ij}^k and serves as a new variable. Instead of directly applying the best response functions (14a) and (14b), we construct the following two optimization problems for solving $\boldsymbol{N}^{vc}$ and $\boldsymbol{N}^{vf}$, respectively.

For contractors, the following modified revenue maximization problem (denoted as RMP thereafter) is developed to solve the distribution of idle contractors $\boldsymbol{N}^{\boldsymbol{vc}}$:

$$\max_{\{T_{ji}^{vc}\ \phi_i^c\}\geq 0\ \{N_i^{vc}\}} \pi^c = \sum_{(i\ j)\in W} F_{ij}\ \ Q_{ij}^0 f(f_w(N_i^{vc}+N_i^{vf})) - M_1^c\ \ \sum_{i\in I}\left(N_i^{vc} - \sum_{j\in J} T_{ji}^{vc}\ \ w_i^{vc}\right) \tag{15a}$$

$$\text{s.t.}\quad \sum_{j\in J} T_{ji}^{vc} = \sum_{j:(i\ j)\in W} Q_{ij}^c\ \ \phi_i^c \quad \forall i \in I \tag{15b}$$

$$\sum_{i\in I} T_{ji}^{vc} = \sum_{i:(i\ j)\in W} Q_{ij}^c\ \ \phi_i^c \quad \forall j \in J \tag{15c}$$

$$\sum_{(i\ j)\in W} Q_{ij}^c\ \ \phi_i^c\ \ \left(h_{ij}+w_i^p\right) + \sum_{j\in J}\sum_{i\in I} T_{ji}^{vc}\ \ h_{ji} + \sum_{i\in I} N_i^{vc} = N^c \tag{15d}$$

$$N_i^{vc} \geq \sum_{j\in J} T_{ji}^{vc}\ \ w_i^{vc} \quad \forall i \in I \tag{15e}$$

$$\phi_i^c \leq M_2^c \quad \forall i \in I. \tag{15f}$$

where M_1^c and M_2^c are large positive numbers with $M_1^c > \max_{i\in I}\{\sum_j F_{ij}\ \partial Q_{ij}(N_i^{vc}\ N_i^{vf})/\partial N_i^{vc}\}$ for any $N_i^{vc} \in [0\ N^c]$ $N_i^{vf} \in [0\ N^f]$ and $M_2^c \gg 1$. Similar to the original platform's optimization problem (13), problem (15) takes market status ζ and the distribution of idle freelancers $\boldsymbol{N}^{vf}$ as inputs and solves $\boldsymbol{N}^{vc}$ and the idle movements of contractors $\{T_{ji}^{vc}\}$ in addition to $\{\phi_i^c\}$. The objective (15a) consists of the platform's expected revenue and a term penalizing the difference between $\sum_{i\in I} N_i^{vc}$ and $\sum_{j\in J}\sum_{i\in I} T_{ji}^{vc}\ \ w_i^{vc}$. The

constraints of problem (15a) resemble those of problem (13) but with inclusions of demand adjusters $\{\phi_i^c\}$ and constraints (15e) and (15f). Among them, constraint (15e) relaxes (7d) as an inequality, and constraint (15f) confines the adjuster to be upper bounded. The above modifications ensure that problem (15) is feasible with $T_{ji}^{vc} = 0\ \forall j \in J\ \ i \in I$, and $\phi_i^c = 0$ and $N_i^{vc} = N^c/|I|\ \forall i \in I$ being a naive feasible solution.

Given market status ζ, freelancers' probability $Pr_{i/j}$ of cruising from a destination zone j to an origin zone i can be determined by Eqs. (3) and (6c). With ζ and $\{Pr_{i/j}\}$, we solve $\boldsymbol{N}^{vf}$ by constructing the following freelancers' customer-searching problem (denoted as FCP for short) that simultaneously accounts for freelancers' strategic repositioning behaviors stated in (14b) and the steady-state conditions (14c):

$$\max_{\{T_{ji}^{vf}\ \phi_i^f\ \delta_i^f\}\geq 0\ \{N_i^{vf}\}} \quad \pi^f = \sum_{(i\ j)\in W} F_{ij}\ \ Q_{ij}^f \phi_i^f - M_1^f\ \ \sum_{i\in I} \delta_i^f \tag{16a}$$

$$\text{s.t.} \quad T_{ji}^{vf} = \sum_{m:(m\ j)\in W} Q_{mj}^f \phi_m^f\ \ Pr_{i/j} \quad \forall j \in J\ \ i \in I \tag{16b}$$

$$\sum_{j\in J} T_{ji}^{vf} = \sum_{j:(i\ j)\in W} Q_{ij}^f \phi_i^f \quad \forall i \in I. \tag{16c}$$

$$\sum_{(i\ j)\in W} Q_{ij}^f \phi_i^f\ \ \left(h_{ij} + w_i^p\right) + \sum_{j\in J}\sum_{i\in I} T_{ji}^{vf}\ \ h_{ji} + \sum_{i\in I} N_i^{vf} = N^f \tag{16d}$$

$$N_i^{vf} = \sum_{j\in J} T_{ji}^{vf}\ \ w_i^{vf} + \delta_i^f \quad \forall i \in I \tag{16e}$$

$$N_i^{vf} \geq \xi \quad \forall i \in I. \tag{16f}$$

where variable δ_i^f represents the difference between the number of idle freelancers N_i^{vf} and $\sum_{j\in J} T_{ji}^{vf}\ \ w_i^v$ for each origin zone $i \in I$. Problem (16) takes $\{Pr_{i/j}\}$ and market status ζ as inputs and solves the spatial distribution of idle freelancers $\boldsymbol{N}^{vf}$, their idle movements $\{T_{ji}^{vf}\}$, and demand adjusters $\{\phi_i^f\}$. Similar to problem (15), the objective (16a) introduces a positive number M_1^f ($M_1^f > 0$) to penalize the term $\sum_{i\in I} \delta_i^f$. Constraints (16b)–(16e) replicates conditions (14b) and (14c) but including additional variables $\{\phi_i^f\}$ and $\{\delta_i^f\}$. The additional constraint (16f) forces N_i^{vf} to be greater than a lower bound ξ at each zone i where $\xi < \frac{N^f}{|I|}$. Problem (16) warrants a feasible solution $T_{ji}^{vf} = 0\ \forall j \in J\ \ i \in I$, and $\phi_i^f = 0$, $N_i^{vf} = \delta_i^f = N^f/|I|\ \forall i \in I$.

We approach the equilibrium solution ($\boldsymbol{N}^{vc}\ \ \boldsymbol{N}^{vf}$) by iteratively updating market status ζ and solving the above two optimization problems. Assembling all calculation process for ζ, $\{Pr_{i/j}\}$, RMP problem (15), and FCP problem (16) essentially leads to the following fixed point problem:

$$\boldsymbol{\Phi} : (\boldsymbol{N}^{vc}\ \ \boldsymbol{N}^{vf}) \rightrightarrows \left\{ (\boldsymbol{N}^{vc}\ \ \boldsymbol{N}^{vf}) \,\middle|\, (3), (6c), (8)\ \ \boldsymbol{N}^{vc} \in \underset{\{\boldsymbol{N}^{vc}\ T_{ji}^{vc}\ \phi_i^c\}}{\operatorname{argmax}}\ \pi^c\ \ \boldsymbol{N}^{vf} \in \underset{\{\boldsymbol{N}^{vf}\ T_{ji}^{vf}\ \phi_i^f\ \delta_i^f\}}{\operatorname{argmax}}\ \pi^f \right\}.$$

It is worth emphasizing that both RMP problem (15) and FCP problem (16) are purely mathematical constructions. Because of the inclusion of demand adjusters $\{\phi_i^k\}$, the intermediate outputs of (15) and (16) could differ from those specified by the best response functions (14a) and (14b) for given ($\boldsymbol{N}^{vc}\ \ \boldsymbol{N}^{vf}$). But as proved by Theorem 1 in Appendix B.1, once a fixed-point solution is found, it would map exactly the MNE conditions (14) along with the platform's optimal repositioning policies for contractors.

Naturally, the above decomposition of the fixed-point problem leads to an iterative solution procedure below.

5.2. Solution procedure

As summarized in Fig. 2, the solution algorithm approaches the MNE by iteratively (a) updating market status ζ; (b) solving RMP problem (15) for the spatial distribution of idle contractors $\boldsymbol{N}^{vc}$ and the platform's centralized repositioning policies; and (c) solving FCP problem (16) for the spatial distribution of idle freelancers $\boldsymbol{N}^{vf}$ and their self-interested repositioning movements. The procedure updates the distributions of idle drivers until convergence.

The detailed solution algorithm is as follows:

1. Initialize ($\hat{\boldsymbol{N}}^{vf}\ \ \hat{\boldsymbol{N}}^{vc}$), M_1^c, M_2^c, and M_1^f;
2. Update ζ through Eqs. (10), (11), and (12);
3. With ζ and $\boldsymbol{N}^{vf}$, obtain $\boldsymbol{N}^{\boldsymbol{vc}}$ and $\{T_{ji}^{vc}\}$ by solving RMP problem (15); With ζ, calculate freelancers' probability $\{Pr_{i/j}\}$ of cruising from j to i through Eqs. (3) and (6c) and obtain $\boldsymbol{N}^{vc}$ and $\{T_{ji}^{vf}\}$ by solving FCP problem (16);
4. If $\sqrt{\sum_{i\in I}(\hat{N}_i^{vc} - N^{vc}) + \sum_{i\in I}(\hat{N}_i^{vf} - N^{vf})} < \varepsilon$, stop the procedure and obtain the solution. Otherwise, update ($\hat{\boldsymbol{N}}^{vc}\ \ \hat{\boldsymbol{N}}^{vf}$) by setting $\hat{\boldsymbol{N}}^{\boldsymbol{vc}}\ \ \boldsymbol{N}^{\boldsymbol{vc}}$ and $\hat{\boldsymbol{N}}^{vf}\ \ \boldsymbol{N}^{\boldsymbol{vf}} + \kappa_s\ \ (\hat{\boldsymbol{N}}^{\boldsymbol{vf}} - \boldsymbol{N}^{\boldsymbol{vf}})$, and return to step 2.

The parameter ε in the above algorithm specifies the error tolerance for convergence. Here, we use a linear combination rule to update $\boldsymbol{N}^{vf}$ and parameter κ_s describes the step size for updating $\boldsymbol{N}^{\boldsymbol{vf}}$ in each iteration. To accelerate the convergence speed, the solution algorithm adopts a self-regulated successive average method where the step size κ_s varies depending on how close the current solution is to the equilibrium solution (Liu et al., 2009).

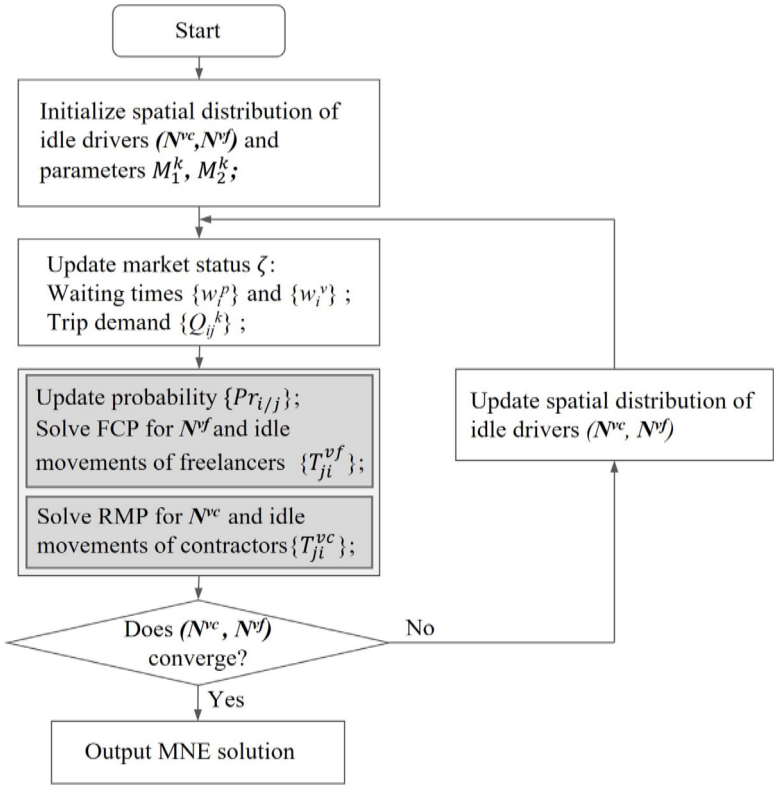

Fig. 2. Solution procedure for calculating MNE.

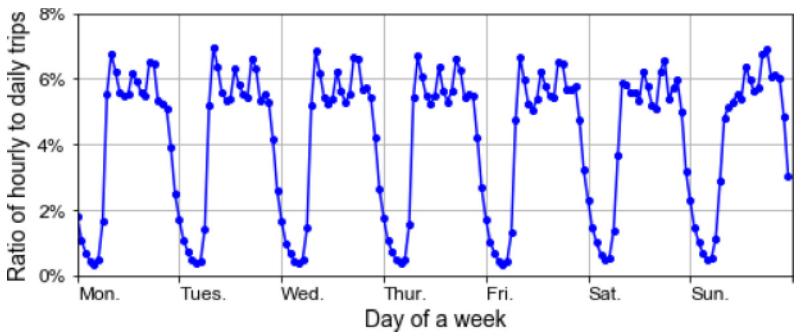

Fig. 3. Demand pattern during the study period.

6. Data for numerical experiments

6.1. Data description

Our datasets come from a major city in China where DiDi as a dominant TNC provides on-demand ride-hailing services. The studied city has been partitioned into 27 zones, including an airport and two railway stations that are distant from the rest spatial market (see Fig. 4).

The raw dataset includes all trip records from a four-week period in 2019 in a granularity of five minutes. In this dataset, we obtain access to each customer's pickup and drop-off locations, the corresponding timestamps when a customer sent out a request, got matched with a driver, got into the car, and completed the trip, as well as the fare charged. On the supply side, the number of occupied and idle drivers in each zone is also available. Fig. 3 displays the aggregated daily demand pattern in a week span, where the request proportion (y-axis) represents the hourly number of trips compared to the total trips in that day. The repetitive shape implies the fairly stable demand pattern across the weekdays.

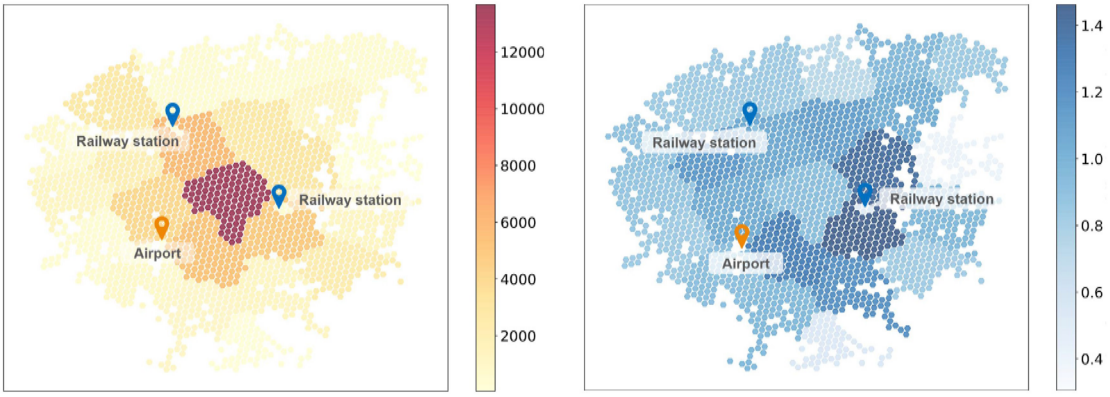

(a) Hourly trip demand (b) Ratios of trip arrival and completion rates

Fig. 4. Spatial demand-supply imbalances at morning peak hours.

Further, Fig. 4 glimpses the spatial imbalance between driver supply and customer demand. As indicated by the contrasts in colors, not only the customer demand level is vastly different across zones, but the market condition, that result from the supply–demand interaction, exhibits substantial heterogeneity with both under-supplied (termed as "hot-spot") and oversupplied (termed as "cold-spot") areas coexisting in the city. Customers in the hot-spot areas may suffer poor quality of service and many trip requests are delayed or rejected by the platform, while drivers in the cold-spot area endure low prolificacy. More importantly, there lacks clear correspondence between the customer demand level and the severity of supply shortage, and thereby stressing the necessity of system/network models to capture the operational cruxes behind.

6.2. Parametric setup and experimental scenarios

Our case study bases on the morning peak period of a typical weekday when spatial supply–demand imbalance appears to be most severe. The realized demand between each OD pair $(i\ j) \in W$, as specified by Eq. (1), is assumed to follow an exponential function:

$$Q_{ij} = Q_{ij}^0 \ \exp\left(\beta \ \ (F_{ij} + \beta_w w_i^p)\right) - \epsilon_{ij} \qquad \forall (i\ j) \in W \tag{17}$$

where the parameter β_w denotes customers' value per unit waiting time; the other parameter β in front of the term $(F_{ij} + \beta_w w_i^p)$ represents each customer's sensitivity to the trip cost of traveling from zone i to j. Customers' in-vehicle travel time is assumed to be constant across the study period and gets embedded in the calibration of potential demand Q_{ij}^0. In accordance with the calibration results from Xu et al. (2021b), the sensitivity parameter β is set to be -0.09 1/CNY, while the value of waiting time β_w anchors at 20 CNY/hour. In Eq. (17), one additional positive parameter ϵ_{ij} is introduced to ensure the satisfaction of regularity conditions C.3. Specifically, setting ϵ_{ij} as $Q_{ij}^0 \ \exp\left(\beta \ \ (F_{ij} + \beta_w \overline{w_i^p})\right)$ ensures that no trips are served when customers' average waiting time reaches their tolerance $\overline{w_i^p}$.

Without matching priority, customers' pickup time function $f_w(\,)$ as prescribed by Eq. (11) is assumed to have the following form:

$$w_i^p = \frac{\eta_i}{\left(N_i^{vc} + N_i^{vf} + \epsilon_1\right)^{\rho}} \qquad \forall i \in I. \tag{18}$$

Here, η_i is a positive parameter that captures the spatial features of zone i; ρ is a non-negative parameter that reflects the efficiency of matching technology; and ϵ_1 is a positive parameter to ensure the boundedness of customers' pickup time (Condition C.2). When the parameter ϵ_1 equals 0, the above equation could be theoretically derived using a first-come-first-serve (FCFS) matching mechanism where each customer is matched with the nearest idle driver (Daganzo, 1978; Zha et al., 2018b). For the case with matching priority, the customers' pickup time function is listed in Appendix D where an additional parameter α_i is included to indicate contractors' matching priority in each zone i.

Customers' pickup times are characterized differently in spot-type areas like airports and train stations versus other spatial zones. The pickup time of customers would decrease with the supply of idle drivers in the spatial markets but remain insensitive in spot-type areas, where ride-hailing vehicles are provided with dedicated waiting areas. Thus, for customer pickup time function, we set $\rho = 0.5$ for the spatial zones (Zha et al., 2018b; Daganzo, 1978) and $\rho = 0.001$ for service spots (Xu et al., 2021b). With further analysis on the empirical data, we set $\eta_i = 0.08$ at the service spots and $\eta_i = 1$ for other spatial zones. The freelancers' initial perception error parameter θ is set to be 0.5 1/CNY.

Table 1
Parameters and their values adopted in the numerical experiments.

Description	Parameter	Value
Fixed parameters across all scenarios	F_{ij} h_{ij}	directly taken from service data
	E_{ij}	$0.8F_{ij}$ (CNY/trip)
	β_w	20 (CNY/hr)
	β	−0.09 (1/CNY)
	γ_1	20 (CNY/hr)
	γ_2	20 (CNY/hr)
	θ	0.5
	$N^c + N^f$	33,000
	η_i	0.08 and 0.1 for spot-type and spatial zones
	ρ	0.001 and 0.5 for spot-type and spatial zones
Baseline scenario	$N^f/(N^f + N^c)$	100
Dual sourcing scenarios without matching priority	α_i	1
	$N^c/(N^f + N^c)$	10% 20% … 100%
Dual sourcing scenarios with matching priority	α_i	0.5 1 1.5 2
	$N^c/(N^f + N^c)$	20% 50%

Note that by specifying customers' trip demand and pickup time as (17) and (18) and setting $\{\epsilon_{ij}\ \epsilon_1\}$ properly, conditions C.1–C.5 hold and hence ensures the existence of MNE as per Theorem 1. Readers can refer to Appendix C for detailed discussions on this matter and on the parametric setting of these parameters.

On the supply side, the total number of active drivers $(N^c + N^f)$ is set at 33,000 to approximate the real-world setting. As per the current practice, freelancers earn 80 percent of trip fares as commission, and the platform keeps the remaining 20 (Chen et al., 2020). Drivers' monetary cost per trip time γ_1 and per idle time γ_2 are assumed to be 20 CNY/hour. We suppose that freelancers are risk-neutral when choosing their target zones. Their perceived trip earning and delivery time, as prescribed by mappings (2), are assumed to be the average weighted trip earning and delivery time given as follows:

$$\hat{E}_i = \frac{\sum_{d:(i\,d)\in W} E_{id}\ \ (Q^f_{id} + \epsilon_2)}{\sum_{d:(i\,d)\in W}(Q^f_{id} + \epsilon_2)} \qquad \hat{h}_i = \frac{\sum_{d:(i\,d)\in W} h_{id}\ \ (Q^f_{id} + \epsilon_2)}{\sum_{d:(i\,d)\in W}(Q^f_{id} + \epsilon_2)} \qquad \forall i \in I$$

where ϵ_2 is a very small positive number to avoid singularity in the cases when denominator $\sum_{d:(i\,d)\in W} Q^f_{id}$ approaches 0.

Throughout the experiments, we take the scenario where freelancers are the sole labor source as the baseline, given it represents the status-quo strategy of labor sourcing for TNCs. Then, we create a set of scenarios by varying the ratio of contractors while keeping the total driver population fixed. Without considering matching differentiation, the implication of dual sourcing is drawn by contrasting the results of dual sourcing equilibrium with that of the baseline scenario (Section 7). Finally, several additional scenarios vary the matching priority of contractors and explore the impact of dual-sourcing matching differentiation policies (Section 8). Table 1 summarizes the parametric settings for the above experimental scenarios.

7. Numerical analysis of dual sourcing

Based on the above settings, this section examines the convergence of the proposed solution algorithm and conducts numerical experiments to examine the impacts of dual-sourcing supply on a ride-hailing system. Specifically, the MNE model is implemented to draw the implications on the dual sourcing and the centralized repositioning of contractors for different service stakeholders, including drivers, customers, and the platform.

7.1. Convergence of the solution algorithm

For type-k drivers, we use the Euclidean norm $\sqrt{\sum_{k\in\{f\ c\}\ i\in I}\left(N_i^{vk(n+1)} - N_i^{vk(n)}\right)^2}$ to measure the convergence gap between two consecutive iterations n and n+1. We illustrate the case with 20 and 50 of active drivers as contractors, and the same convergence pattern applies to other percentages. Fig. 5(a) illustrates the convergence gap with iterations. There, each line differs from others in the initial values for $\boldsymbol{N}^{vk}$ that are used in calculating MNE solutions. As shown in Fig. 5, the convergence gaps decrease rapidly within hundreds of iterations in all cases.

7.2. Impact on drivers and customers' service experiences

We first consider the impact of dual sourcing on supply utilization by examining three scenarios where contractors make up 0 , 20 , and 50 of the total driver population, respectively. Fig. 6 compares the proportions of drivers' labor hours over the four service states, namely customer delivery, pickup, repositioning, and waiting for matching, under the three mixed equilibria. Among the four service states, in particular, the time spent in delivery is metered and thus considered as being effectively utilized. Despite the three separate cases, it is clear that with the increasing share of contractors, the percentage of the time that drivers

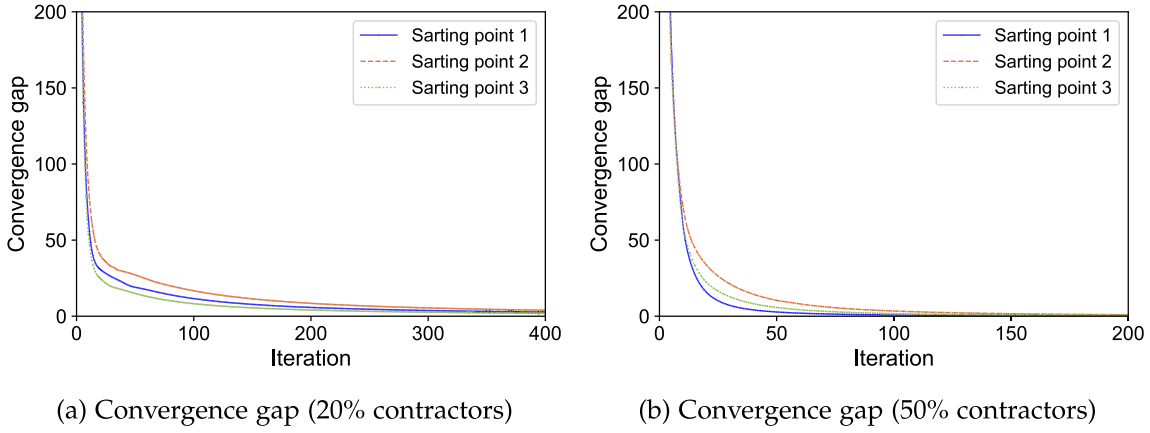

Fig. 5. Convergence gap over iterations.

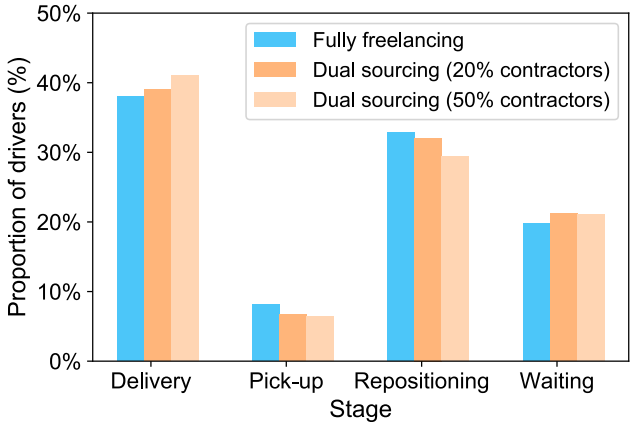

Fig. 6. The proportion of drivers in each service stage at mixed equilibria.

spend delivering customers mildly goes up whereas those in pickup and repositioning stages reduce significantly. Even though the waiting time of drivers in matching increases, this contributes to the reduction of the pickup time (as implied by the pickup time function (11)). Overall, given the fixed number of drivers in total, the labor supply of drivers is utilized more efficiently with the increasing composition of contractors who follow the platform's repositioning guidance.

We then move to the realized demand profile by varying the proportion of contractors in a higher granularity from 0 to 100 with a step of 10 . Fig. 7 summarizes the changes of the total realized demand and the corresponding shares fulfilled by contractors and freelancers. Specifically, Fig. 7(a) indicates that converting drivers from freelancers to contractors can boost the demand by up to 4 . However, the marginal return is observed to be diminishing overall. The first 20 contractual conversion gives rise to the most significant pickup in the demand volume, whereas further increasing the share of contractors yields lacklustre increments. A similar phenomenon can be observed in Fig. 7(b). For mixed fleets with contractors composing less than 50 , individual contractors are directed to undertake slightly more trips exceeding their freelancer counterparts. But when contractors compose more than half of the labor supply, their task loads become no different from that of freelancers. In fact, the interest of freelancers and the platform is not entirely contradictory. The will of an individual freelancer for higher earnings would benefit the platform in higher revenues and trip demand as well. Such partially aligned interest thus weakens the necessity of a pure-contractor strategy for TNC platforms, especially when the cost of retaining contractors appears higher than freelancers.

Besides, contracting with a subgroup of drivers may raise the concern that dual sourcing would intensify the competition and reduce freelancers' expected payoff. To look into this potential issue, Fig. 8(a) compares the average number of trips served per freelancer and contractor across the mixed equilibria over the different proportions of contractors. Without prioritizing any driver group in matching, the results suggest that converting some drivers to contractors will not necessarily adversely affect the trips served by freelancers. Interestingly, when the proportion of contractors surpasses 60 , the number of trips served by the freelancers will increase whereas that of contractors gradually declines. A similar pattern is also presented in Fig. 8(b) on the effective hourly wage of freelancers. There lack of a sign that involving contractors could systematically undermine the wages of freelancers. Meanwhile, since contractors are paid with fixed salaries, the platform needs to balance labor costs and the expansion of service capacity. Fig. 8(b)

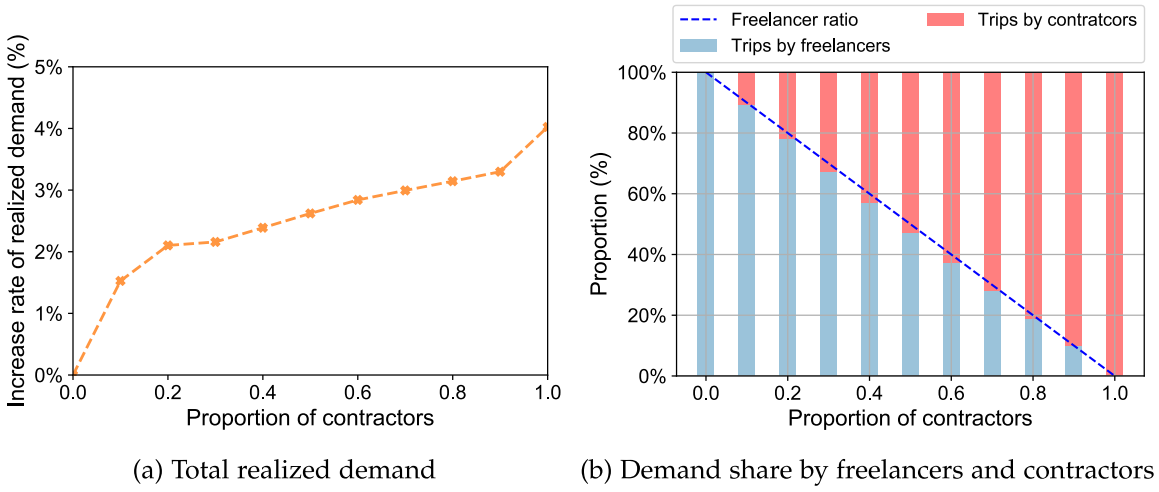

(a) Total realized demand (b) Demand share by freelancers and contractors

Fig. 7. System realized demand under different proportions of contractors.

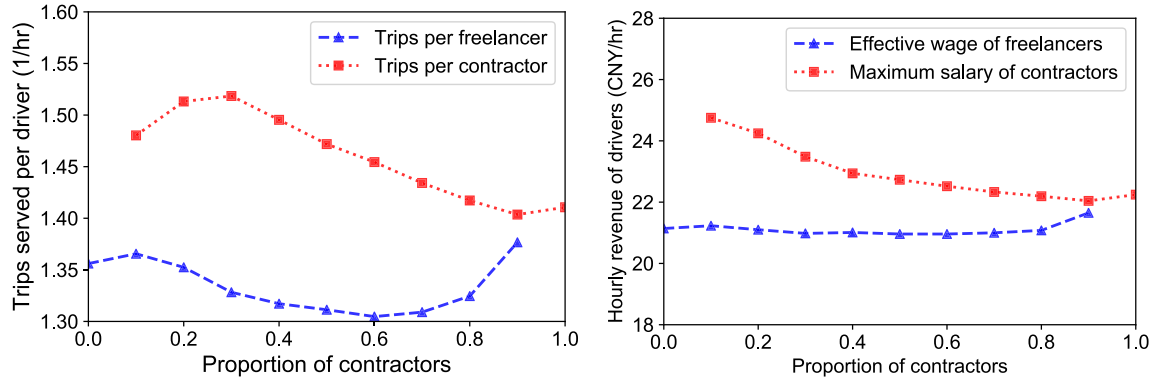

(a) Trips per driver (b) Freelancers′ wage and highest salary

Fig. 8. Trips served per driver and corresponding hourly revenue.

plots the platform's willingness to pay contractors (namely, the maximum salary) for achieving positive profit margins compared to the status quo. As shown, the platform's willingness to pay steadily decreases as the proportion of contractors increases and eventually overlaps with the effective wage of freelancers. This again marks the diminishing marginal return for converting drivers from freelancers to contractors. In particular, when a platform needs to pay contractors with a salary higher than the commission that they would receive under the freelance agreement, the best strategy is to stick with the mixed supply composition.

We caution that the above conclusions are drawn with the assumption of an indiscriminate matching policy. Later, Section 8 sheds light on how matching priority may affect drivers' payoffs.

7.3. Impacts on the platform's profit

TNC platforms adopt dual sourcing expecting that the more obedient contractors could increase the overall profitability. Suppose a platform offers contractors a guaranteed hourly salary s. The platform's profit is thus defined as its revenue π (given by Eq. (13a)) minus the total labor cost $\sum_{(i\,j)\in W} E_{ij} Q_{ij}^{f} + s\ N^{c}$. Note that the profit margin of contractual conversion from freelancers to contractors depends on the driver composition and the risk-free salary for contractors. In practice, the design of contractors' salaries manifest the trade-off between the benefits of risk-hedging and the limitation in free service provision. Here, we examine a set of hypothetical scenarios coupling the two dimensions of system settings: (a) Ten levels of supply composition with the proportion of contractors ranging from 0 to 100 by a step of 10 ; (b) Four levels of hourly salary s for contractors respectively anchoring at 5 and 10 reduction/surge based on freelancers' status-quo hourly earning r_0. Conceptually, the conditions of s being greater or less than r_0 refer to the cases when the market exhibit high or low uncertainty to drivers, respectively (Dong et al., 2021).

The platform's profits across the different scenarios are summarized in Fig. 9, where the y-axis shows the percentage change in profit compared to the status quo, i.e., a pure-freelancer case. The upward trends presented by the top two curves imply that when

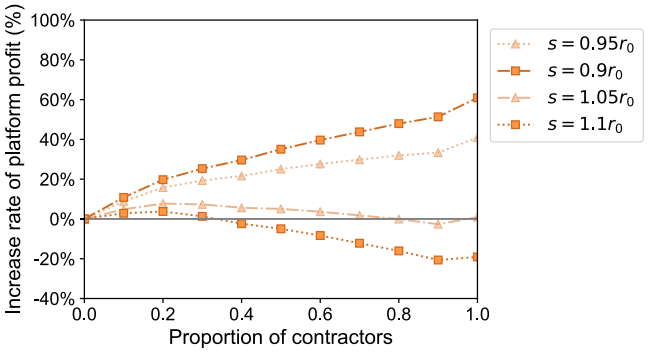

Fig. 9. Platform's profit versus the proportion of contractors.

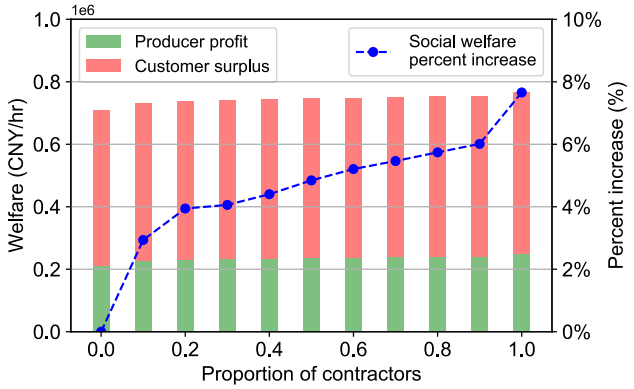

Fig. 10. Social welfare versus the proportion of contractors.

there appears relatively high market uncertainty and thus low cost for contractor recruitment, the platform could be in favor of a pure-contractor structure to service more trips at competitive labor costs. But as the salary paid to contractors goes up, the platform would prefer a mixed supply composition with low penetration of contractors, who would then act as system actuators. In these circumstances, the diminishing return of converting freelancers into contractors cannot stay profitable with a high penetration of contractors. Such a result echoes what has been concluded previously.

7.4. Impact on social welfare

Since the number of drivers is assumed to be fixed, the social welfare sums up the customers' surplus and the producers' profits. The customers' surplus C_s is calculated by the following formula:

$$C_s = \sum_{(i\ j)\in W} \int_0^{Q_{ij}} \frac{1}{\beta} \ln \frac{x}{Q_{ij}^0} \mathrm{d}x - \sum_{(i\ j)\in W} \left(F_{ij} + \beta_w w_i^p\right) \quad Q_{ij}$$

where the inverse demand function is adapted from Eq. (17). Meanwhile, the producers' profits P_s add up those from the platform, freelancers, and contractors,

$$P_s = \sum_{(i\ j)\in W} Q_{ij} \quad F_{ij} - \gamma_1 \quad (N^c + N^f)$$

where in the right-hand side the first term represents the producers' total revenue and the latter two terms denote drivers' trip cost of picking up and delivering customers, idle repositioning, and waiting to be matched.

Fig. 10 shows that both the customers' surplus and the producers' profits increase monotonically as the penetration of contractors enlarges. Specifically, the adoption of dual sourcing increases the consumers' surplus by up to 4 , proportional to the realized customer demand. The demand surge further accelerates the circulation of drivers in service, thereby stimulating the total profits earned by producers. In sum, the deployment of dual sourcing can increase social welfare by up to 8 . Thus, while a higher proportion of contractors may not appear tempting to the platform, it does benefit the entire system with higher social welfare.

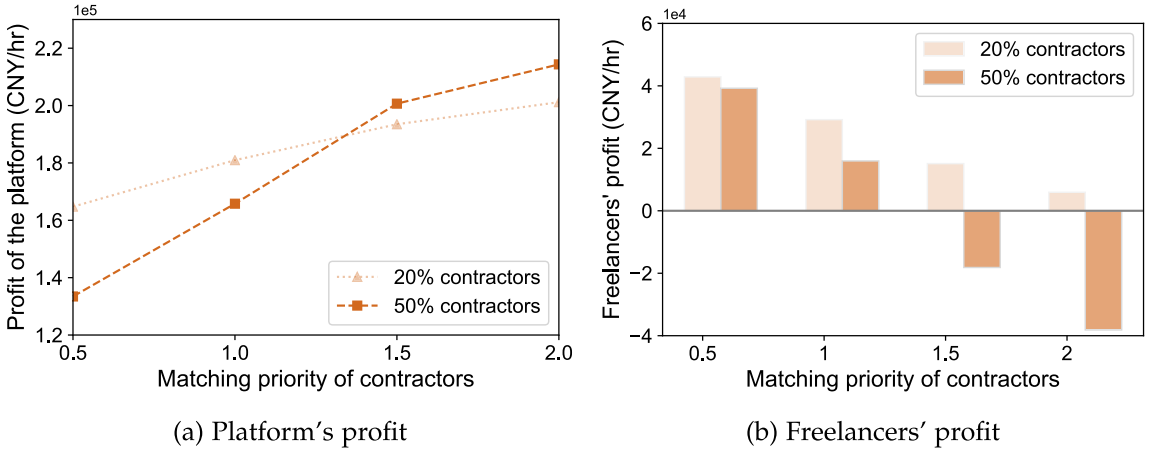

Fig. 11. Platform and freelancers' profits under different levels of matching priority.

8. MNE with matching priority

The previous sections assume that the platform treats freelancers and contractors equally in matching. It is notable that instituting matching priority/discrimination dependent on varying contractual types can directly affect drivers' expected payoff and indirectly influence their movement over the network. This section relaxes the equal-treatment assumption by expanding the MNE model with a more general module that allows region-specific matching priority. The implications of matching priority under the dual-sourcing context are analyzed numerically via various service performance measures.

Keeping the rest components unchanged, the MNE replaces the matching module with one that permits matching priority. Suppose the platform still enforces a distance-based matching scheme. Then, the matching priority can be implemented through distance-adjustment factors applied to certain groups of drivers. Without loss of generality, we set contractors as the base group that maintains the actual distance measures. Now, let r represent the actual distance between a customer and her nearest idle contractor, and α_i be the distance-adjustment ratio for freelancers. Then, the customer would be matched to the contractor only if there are no idle freelancers in the vicinity of r/α_i. Accordingly, the condition of α_i being greater(less) than 1 refers to the matching policies that prioritize(discriminate) contractors. The adjustment factors can be region-specific, thereby being flexible of covering various priority policies under this framework.

The mathematical derivation of group-specific matching probabilities and pickup time for freelancers and contractors under the above mechanism is included in Appendix D, while the rest of this section focuses on the analysis of yielded mixed equilibria. The effects of matching priorities are evaluated under two typical schemes that differ in their spatial granularity in implementation. A uniform scheme adopts a homogeneous matching priority across the entire network, whereas a fine-grained scheme enables the platform to tailor the degrees of priority for specific zones.

8.1. Effects of spatially uniform schemes

For a uniform scheme, drivers under each contractual type experience universal matching priority in all zones $i \in I$. Here, we set the distance-adjustment ratio α_i at four levels of $\{0.5\ 1\ 1.5\ 2\}$, which respectively stand for (a) prioritizing freelancers, (b) equal treatment, (c) slightly prioritizing contractors, and (d) heavily prioritizing contractors. For demonstration purposes, we consider two contexts with contractors constituting 20 and 50 of the driver population receiving a risk-free salary s of $1.1r_0$.

Fig. 11 presents the profits that the platform and freelancers receive in response to the different levels of matching priority. Some useful insights can be obtained from the sets of comparisons. First, based on Fig. 11(a), it is clear that given the total supply, prioritizing contractors who follow centralized repositioning guidance can constantly benefit the platform. But in the meanwhile, elevating the penetration of contractors could impose contrasting effects that do not always benefit the platform. The platform can only expect higher profit from involving more contractors when they receive adequate priority in matching. Otherwise, the centralized repositioning is insufficient in compensating for the higher cost incurred by the recruitment of contractors. Besides, in contrast to the platform's rising profits, Fig. 11(b) suggests that freelancers' profit declines dramatically with respect to contractors' matching priority. At a medium penetration of contractors in the labor supply, freelancers' average profit slides underneath zero even if the platform only prioritizes contractors slightly. Such a great sensitivity of profit migration among drivers in response to the matching priority alerts ride-hailing platforms who consider to take prioritizing policies for contractors. Even slight matching discrimination against certain driver groups can severely drag down their profitability, potentially exclude them out of the market, and eventually worsen the system supply.

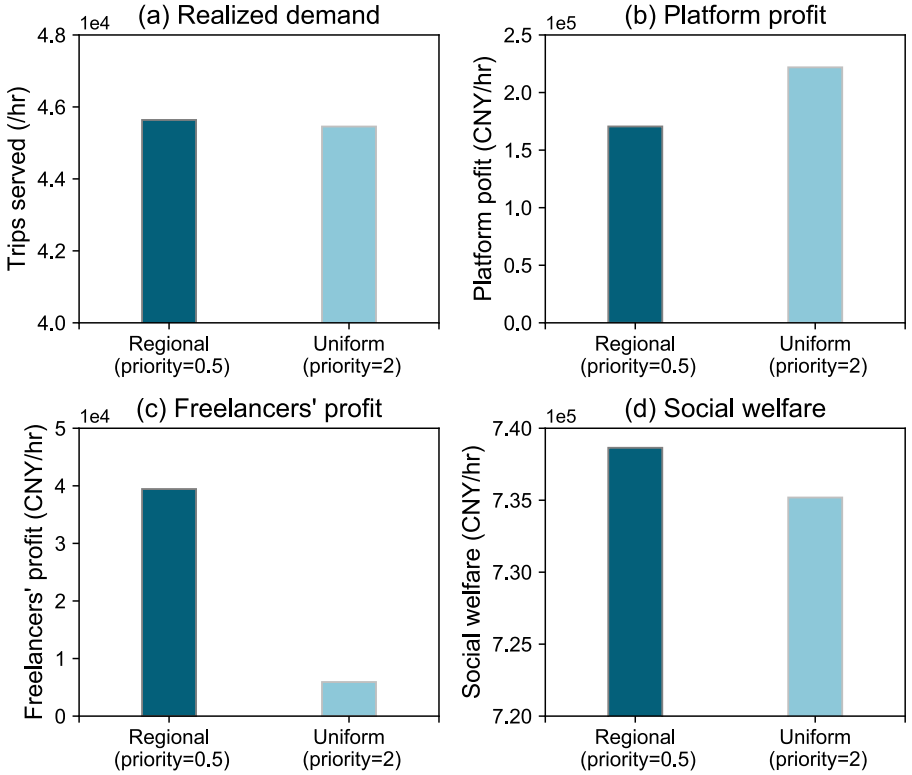

Fig. 12. Comparison of two schemes that conceptualize spatially uniform and heterogeneous matching priority (assuming 20 contractor penetration).

8.2. *Effects of spatially heterogeneous schemes*

The above results illustrate that uniform matching priority schemes can be abused and give rise to unfavorable system outcomes for either the platform or freelancers. However, such adverse effects should not be understood as evidence for completely abandoning the use of matching priority. Through the following example, we showcase that differentiated matching, if implemented regionally at specific areas, can serve as an extraordinary option for supply management.

Since freelancers reposition with self-interest, an area with reduced waiting time for freelancers could incentivize more cohorts to service there. We investigate a naive scheme that sets the adjustment ratio α_i at 0.5 in the central downtown of the city (i.e., the purple area in the center of Fig. 4(a)) but keeps it as 1 among all other regions. Accordingly, the platform prioritizes freelancers in the downtown while treating the two types of drivers equally elsewhere. Interestingly, the overall system performance under such a simple priority scheme is comparable to that of a universal counterpart where contractors are heavily prioritized in matching (with $\alpha_i = 2$ for all $i \in I$). As revealed by Fig. 12, the regional priority scheme attains a very similar level of realized demand while going slightly higher in the social welfare and lower in the platform's profit, compared to the uniform scheme. But meanwhile, the former scheme is able to secure significantly higher profits for freelancers and thus appears to be superior in sustaining the labor supply for the service. Such an outcome showcases the favorable use of contractors as system actuators that effectively complement the primary labor source of freelancers. To fully exploit the advantages of dual sourcing, a platform could consider integrated designs of matching and repositioning for contractors.

9. Conclusion and future work

This paper investigates the impacts of dual-sourcing strategy in a ride-hailing market, where drivers can either serve as freelancers or contractors. The idea is to leverage contractors, who follow the platform's strategic guidance, as system actuators to neutralize the self-interested service behavior of freelancers and mitigate the spatial mismatch between demand and supply. An MNE model is developed to capture the interplay between freelancers' and contractors' repositioning movements, with a fixed-point iterative method devised for equilibrium solutions and the platform's repositioning policies in a general network context. We provide a theoretical proof for the existence of mixed network equilibrium. Numerical experiments and sensitivity analysis are conducted based on real-world cases from Didi Chuxing. Below summarize the major findings surrounding the implementation of dual sourcing in supply management:

Given the total number of drivers in service, converting drivers from freelancers to contractors can constantly increase the realized demand and the total social welfare. However, once contractors' penetration exceeds 20 of the driver population, their marginal value diminishes significantly.

The platform's profit is sensitive to the salary paid to contractors. When contractors are less costly to recruit than freelancers, the platform favors a pure contractor structure. Otherwise, only the dual sourcing strategy with a thin penetration of contractors would remain profitable.

Matching priority should be implemented with caution. A uniform priority scheme for contractors can be abused with catastrophic consequence toward freelancers, whereas a fine-grained scheme with differentiated matching ratio tailored at local regions can better promote the facilitating role of contractors in dual sourcing.

Future research could extend along the following avenues. First, our work considers a static network equilibrium, while the ride-hailing market in practice characterizes more transient market states. Consequently, the effects of dual sourcing strategy might be underestimated. Extending the model to a dynamic context is meaningful and could be accomplished in various ways. For example, characterizing the system dynamics and state transitions with dual sources can be a straightforward extension. Beyond that, we may consider drivers' time- and state-dependent utility and investigate how freelance drivers' far-sighted repositioning behaviors influence the platform's optimal repositioning policy for contractors. Appendix E discusses the extensions toward dynamic settings in more detail. Second, this paper primarily focuses on the use of contractors in strategic repositioning, with preliminary discussions provided on differentiated matching. It is of great importance to explore the joint optimization of repositioning and other operational policies, especially more sophisticated ones like ride pooling. Last but not least, the conclusions resulting from the counterfactual analyses should be carefully validated as more relevant data becomes available.

As a closing remark, this study can offer insight into the management of mixed-autonomy systems, in which autonomous vehicles can be viewed as centralized contractors and human-driven vehicles as freelancers. The proposed MNE framework can be used to analyze the effects of increasing the fraction of autonomous vehicles on human drivers, as well as the effects of a mixed-autonomy strategy on improving service quality. It would be advantageous to expand the current framework to include automation factors such as fairness concerns and cleaning needs.

Declaration of competing interest

The authors declare that they have no known competing financial interests or personal relationships that could have appeared to influence the work reported in this paper.

Data availability

The GAMS source code utilized for the numerical analysis in this study, along with the parametric input values, can be accessed through the following link: https://gwu.box.com/s/1vw7jsay9ufwphv60n47pk4cun26myfu. Interested researchers can download the materials to replicate the study's findings or to conduct further analysis.

Acknowledgments

The work described in this paper was partly supported by research grants from the National Science Foundation, United States (CMMI-1854684; CMMI-1904575) and DiDi Chuxing. Jian Wang thanks the support of National Natural Science Foundation of China (No. 91846301).

Appendix A. Nomenclature

Notation	Description
Sets	
I	Set of customers' origin zones
J	Set of customers' destination zones
W	Set of OD pairs
Variables	
w_i^p	Customers' average waiting time in zone i (hr)
w_i^{vk}	Average waiting time of type-k drivers in zone i (hr)
N_i^{vk}	Number of idle type-k drivers in zone i
Q_{ij}	Realized service demand for OD pair $(i\ j) \in W$ (trips/hr)
Q_{ij}^k	Trips between OD pair $(i\ j)$ served by type-k drivers (trips/hr)
T_{ji}^{vk}	Idle repositioning flow of type-k drivers from zone j to i (1/hr)
U_{ji}	Freelancers' utility for repositioning from zone j to i (CNY)
$\hat{E}_i$	Average earning of drivers at zone i (CNY)
$\hat{h}_i$	Average en-route time for trips originating from zone i (hr)
N^k	Number of type-k drivers in service
P_i^k	Customers' probability of matching with type-k drivers at zone i

Parameters	
Q_{ij}^0	Potential trip demand from zone i to j (trips/hr)
F_{ij}	Trip fare from zone i to j (CNY/trip)
E_{ij}	Freelancers' earning per completed trip from zone i to j (CNY/trip)
h_{ij}	Trip duration from zone i to j (hr)
β_w	Customers' value per unit waiting time (CNY/hr)
β	Customers' sensitivity to the trip cost (1/CNY)
γ_1	Drivers' value per unit travel time (CNY/hr)
γ_2	Drivers' value per unit idle time (CNY/hr)
α_i	Adjustment ratio for freelancers' relative matching priority in zone i
η_i	Positive parameter in the pickup time function for zone i
ρ_i	Non-negative ratio in the pickup time function for zone i
θ	Degree of drivers' perceptual dispersion over utility
s	Salary for contractors (CNY)
ϵ_{ij}	An adjustment parameter in trip demand function
ϵ_1	A positive parameter in pick-up time function
ϵ_2	A positive parameter to avoid singularity when calculating $\hat{E}_i$ and $\hat{h}_i$
unctions	
$f(\,)$	Function of customer demand in response to the waiting time
$f_w(\,)$	Function of customers' pickup time on the number of idle drivers
$G_e(\,)$	Mapping for drivers' perceived earning from customer trips
$G_h(\,)$	Mapping for average delivery time of customer trips

Appendix B. Supplementary proofs for Section 4

B.1. Proof on the existence of market equilibrium

We prove the following market equilibrium existence theorem by Kakutani's fixed point theorem.

Theorem 1 (*Existence of Mixed Network Equilibrium*). *If conditions C.1–C.6 are satisfied, there exists at least one equilibrium solution to the MNE model defined by (14).*

The solution procedure in Section 5 creates a mapping $\boldsymbol{\Phi}: (\boldsymbol{N}^{vc}\ \boldsymbol{N}^{vf}) \rightrightarrows (\boldsymbol{N}^{vc}\ \boldsymbol{N}^{vf})$ in the following steps: (1) Given $(\boldsymbol{N}^{vc}\ \boldsymbol{N}^{vf})$, the mapping $\boldsymbol{\Phi}$ updates the market status ζ characterized by customers' average waiting time $\{w_i^p\}$, trip demand $\{Q_{ij}^k\}$, and drivers' average waiting time $\{w_i^{vk}\}$. (2) With ζ as input parameters, the optimization problems (15) and (16) output $\boldsymbol{N}^{vc}$ and $\boldsymbol{N}^{vf}$, respectively.

Fig. 13 outlines the roadmap for proving the existence of fixed points satisfying the MNE condition. As depicted, Lemma 1 first establishes a lower bound ξ for freelancers' idle supply $\boldsymbol{N}^{vf}$, with which the mapping space for $\boldsymbol{\Phi}$ can be constructed. Lemma 2 then investigates the existence of strictly positive solutions to problem (16) and deduces the continuity properties for mapping $\boldsymbol{\Phi}$ as presented in Proposition 1. Finally, given the results of Lemmas 1, 2, and Proposition 1, Theorem 1 proves that the mapping $\boldsymbol{\Phi}$ has at least one fixed point by applying Kakutani's fixed point theorem.

B.1.1. Preliminary lemmas and propositions

Step 1. Recall that the existence of MNE solution $(\boldsymbol{N}^{vc}\ \boldsymbol{N}^{vf})$ requires the satisfaction of conditions (14a), (14b) and (14c). As the first step, the following Lemma 1 proves the existence of a lower bound ξ for freelancer's supply N_i^{vf} when (14b) and (14c) are satisfied.

Lemma 1. *For any given $N_i^{vc} \in [0\ N^c]\ \forall i \in I$, there exists a bound $\xi > 0$ such that $N_i^{vf} \geq \xi\ \forall i \in I$ holds for any solution $\boldsymbol{N}^{vf}$ that solves (14b) and (14c).*

Proof. Taking $\boldsymbol{N}^{vc}$ as inputs, (14b) and (14c) solves for the tuple $(\{Q_{ij}^f\}\ \{w_i^p\}\ \{w_i^{vf}\}\ \boldsymbol{N}^{vf}\ \{T_{ji}^{vf}\}, \{U_{ji}\}\ \{Pr_{i/j}\})$ from the following system of equations:

$$w_i^p = f_w(N_i^{vc} + N_i^{vf}) \quad \forall i \in I \tag{19a}$$

$$Q_{ij}^f = Q_{ij}^0\ \ f\left(w_i^p | F_{ij}\ h_{ij}\right)\ \ \frac{N_i^{vf}}{N_i^{vf} + N_i^{vc}} \quad \forall (i\ j) \in W \tag{19b}$$

$$T_{ji}^{vf} = \sum_{m:(m\ j)\in W} Q_{mj}^f\ \ Pr_{i/j} \quad \forall j \in J\ \ i \in I \tag{19c}$$

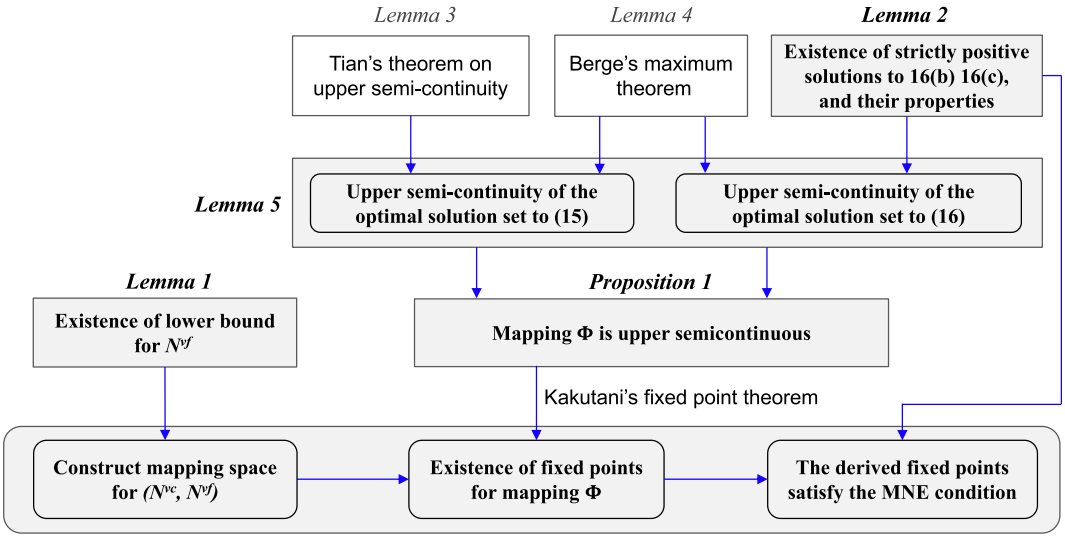

Fig. 13. Proof roadmap for Theorem 1 on the existence of mixed network equilibrium with dual sourcing.

$$\sum_{j\in J} T_{ji}^{vf} = \sum_{j:(i\ j)\in W} Q_{ij}^{f} \quad \forall i \in I \tag{19d}$$

$$\sum_{(i\ j)\in W} Q_{ij}^{f} \left(h_{ij} + w_i^{p}\right) + \sum_{j\in J}\sum_{i\in I} T_{ji}^{vf} \left(h_{ji} + \sum_{i\in I} N_i^{vf}\right) = N^{f} \tag{19e}$$

$$N_i^{vf} = \sum_{j\in J} T_{ji}^{vf} \left(w_i^{vf}\right) \quad \forall i \in I \tag{19f}$$

$$Pr_{i/j} = \frac{\exp(\theta U_{ji})}{\sum_{m\in I}\exp(\theta U_{jm})} \quad \forall i \in I\ j \in J \tag{19g}$$

$$U_{ji} = G_e\left(\{E_{id}\ Q_{id}\}_{d:(i\ d)\in W}\right) - \gamma_1 \left(h_{ji} + G_h\left(\{h_{id}\ Q_{id}\}_{d:(i\ d)\in W}\right)\right) - \gamma_2 \left(w_i^{vf}\right). \tag{19h}$$

Given any $N_i^{vc} \in [0\ N^c]\ \forall i \in I$, solving the above system of equations can be reduced to solve a special case of the fixed point problem with respect to $\boldsymbol{N}^{vf}$ in Xu et al. (2021b). Specifically, according to Eqs. (19a) and (19b), applying $\boldsymbol{N}^{vc}$ and $\boldsymbol{N}^{vf}$ uniquely determines customers' average waiting times $\{w_i^p\}$, and the demand served by freelancers $\{Q_{ij}^f\}$. Next, freelancers' average waiting time $\{w_i^{vf}\}$ and idle vehicle flow $\{T_{ji}^{vf}\}$ are obtained by solving a convex optimization (Wong and Yang, 1998; Xu et al., 2021b). Plugging $\{w_i^{vf}\}$ and idle flow $\{T_{ji}^{vf}\}$ into Eq. (19f), we obtain $\boldsymbol{N}^{vf}$, which are feasible solutions to the fixed point problem under Condition C.3.

Given the number of idle contractors N_i^{vc}, let $\underline{N}_i^{vf}(N_i^{vc})$ denote the lower bound for N_i^{vf} satisfying system of Eqs. (19a)–(19h). Let $\xi = \inf \Xi$ denotes a global lower bound where Ξ is a set comprising $\underline{N}_i^{vf}(N_i^{vc})$ for all zone $i \in I$ and $N_i^{vc} \in [0\ N^c]$. Recall that freelancers' utility U_{ji} satisfies the following formula by Eq. (19h),

$$\min_{(i\ d)\in W}\{E_{id}\} - \gamma_1 \left(h_{ji} + \max_{(i\ d)\in W}\{h_{id}\}\right) - \gamma_2 \left(w_i^{vf}\right) \le U_{ji} \le \max_{(i\ d)\in W}\{E_{id}\} - \gamma_1 \left(h_{ji} + \min_{(i\ d)\in W}\{h_{id}\}\right)$$
$$\forall j \in J\ i \in I. \tag{20}$$

In the above inequality, freelancers' average waiting time w_i^{vf} can be expressed as $w_i^{vf} = N_i^{vf} / \sum_{j:(i\ j)\in W} Q_{ij}^f$ through Eqs. (19d) and (19f), because $\boldsymbol{N}^{vf} > \boldsymbol{0}$ holds at the fixed point. Then, as per Condition C.5, w_i^{vf} has an upper limit $\overline{w}_i^{vf}$ for given $N_i^{vc} \in (0\ N^c]$ and $N_i^{vf} \in (0\ N^f]$. Therefore, for any $j \in J$ and $i \in I$, inequality (20) suggests the existence of common bounds $[\underline{U}\ \overline{U}]$ for U_{ji}, i.e.,

$$\begin{cases} \underline{U} = \min_{(i\ d)\in W}\{E_{id}\} - \gamma_1 \left(h_{ji} + \max_{(i\ d)\in W}\{h_{id}\}\right) - \gamma_2 \left(\overline{w}_i^{vf}\right) \\ \overline{U} = \max_{(i\ d)\in W}\{E_{id}\} - \gamma_1 \left(h_{ji} + \min_{(i\ d)\in W}\{h_{id}\}\right). \end{cases}$$

Since $U_{ji} - U_{jm} \le \overline{U} - \underline{U}\ \forall m \in I$, and freelancers' routing probability $Pr_{i/j}$ can expressed as $Pr_{i/j} = 1/\sum_{m\in I}\exp(\theta U_{jm} - \theta U_{ji})$ $\forall j \in J\ i \in I$ by Eq. (19g), a lower bound $\underline{Pr}_{i/j}$ for $Pr_{i/j}$ can be given as

$$\underline{Pr}_{i/j} = \frac{1}{|I|\ \exp(\theta\overline{U} - \theta\underline{U})} \quad \forall j \in J\ i \in I.$$

Finally, to satisfy (14b) and (14c), we have Eqs. (19d), (19e) and (19f) give rise to the following inequality,

$$\sum_{(i\ j)\in W} Q_{ij}^{f} \left(h_{ij} + w_i^{p}\right) + \sum_{j\in J}\sum_{i\in I} T_{ji}^{vf} \left(h_{ji} + w_i^{vf}\right) \le \sum_{(i\ j)\in W} Q_{ij}^{f} \left(2\overline{h} + \overline{w}_i^{p} + \overline{w}_i^{vf}\right)$$

where $\overline{h} = \max_{i\in I}\max_{j\in J}\{h_{ij}\ h_{ji}\}$; and $\overline{w}_i^p$ denotes the common upper bounds for customers' average waiting time, which exists given inputs $\boldsymbol{N}^{vc} + \boldsymbol{N}^{vf} \geq \boldsymbol{0}$ (Condition C.2). The above inequality then leads to the following formula, i.e.,

$$\sum_{(i\ j)\in W} Q_{ij}^f \geq \frac{N^f}{2\overline{h} + \overline{w}_i^p + \overline{w}_i^{vf}}. \tag{21}$$

Combining inequality (21) with Eqs. (19c) and (19d), we have

$$\sum_{j:(i\ j)\in W} Q_{ij}^f = \sum_{j\in J} T_{ji}^{vf} = \sum_{j\in J}\sum_{m:(m\ j)\in W} (Pr_{i/j}\ \ Q_{mj}^f) \geq \underline{Pr}_{i/j}\ \ \frac{N^f}{2\overline{h} + \overline{w}_i^p + \overline{w}_i^{vf}} \qquad \forall i \in I. \tag{22}$$

Recall that Q_{ij}^f changes continuously with N_i^{vf} for given $N_i^{vc} \geq 0$ and satisfies $\sum_{j:(i\ j)\in W} Q_{ij}^f \to 0$ as $N_i^{vf} \to 0$ (Eqs. (19a), (19b) and Condition C.3). Thus, there must exist a lower bound $\underline{N}_i^{vf} > 0$ such that $\sum_{j:(i\ j)\in W} Q_{ij}^f = \underline{Pr}_{i/j}\ \ N^f / \left(2\overline{h} + \overline{w}_i^p + \overline{w}_i^{vf}\right)$ holds for any $N_i^{vc} \in [0\ \ N^c]$. This concludes the existence of a lower bound $\xi > 0$ for $\boldsymbol{N}^{vf}$. □

Step 2. Lemma 2 explores the solution properties of the system of Eqs. (16b) and (16c), serving as the basis for the freelancers' problem (16).

Lemma 2. *Consider the system of equations formed by (16b), (16c) and the following equation:*

$$\sum_{(i\ j)\in W} Q_{ij}^f \phi_i^f\ \ \left(h_{ij} + w_i^p\right) + \sum_{j\in J}\sum_{i\in I} T_{ji}^{vf}\ \ \left(h_{ji} + w_i^{vf}\right) = L > 0 \tag{23}$$

Then, given that $\{h_{ij}\}$, $\{h_{ji}\}$, $\{w_i^{vf}\}$, $\{Q_{ij}^f\}$, $\{Pr_{i/j}\}$, and $\{w_i^p\}$ are positively valued, there exists one unique solution $(\{T_{ji}^{vf}\}\ \{\phi_i^f\})$ to the above system of equations satisfying the following conditions:

- *A The solution is strictly positive, i.e., $T_{ji}^{vf} > 0\ \forall j \in J\ \ i \in I$ and $\phi_i^f > 0\ \forall i \in I$.*
- *B Assume that L renders a unique solution $(\{T_{ji}^{vf(L)}\}\ \{\phi_i^{f(L)}\})$. Then, for any arbitrary $\varrho > 0$, ϱL renders the solution $(\{T_{ji}^{vf(\varrho L)}\}\ \{\phi_i^{f(\varrho L)}\}) = (\{\varrho T_{ji}^{vf(L)}\}\ \{\varrho\phi_i^{f(L)}\})$.*

Proof. The above system of equations has $(|I| \times |J| + |I|)$ unknowns and $(|I| \times |J| + |I| + 1)$ equations. Note that the cruising probability satisfies $\sum_{i\in I} Pr_{i/j} = 1$ for any destination $j \in J$. There exists a redundant equality because

$$\sum_{i\in I}\sum_{j\in J} T_{ji}^{vf} = \sum_{j\in J}\{\sum_{i\in I} Pr_{i/j}\ \ (\sum_{m:(m\ j)\in W} Q_{mj}^f \phi_m^f)\} = \sum_{j\in J}\sum_{m:(m\ j)\in W} Q_{mj}^f \phi_m^f = \sum_{i\in I}\sum_{j:(i\ j)\in W} Q_{ij}^f \phi_i^f.$$

Since $\{Q_{ij}^f\}$ and $\{Pr_{i/j}\}$ are positive, one can eliminate one redundant equation from (16c) such that the remaining equations are linearly independent.

We apply Farkas' lemma to prove that the solution to the above system of equations is non-negative. Let $\mathcal{A}$ denote a $n \times n$-dimensional coefficient matrix, and $\boldsymbol{b}$ be an n-dimensional column vector with $n = (|I| \times |J| + |I|)$. For simplicity, we use r to denote the index thereafter, i.e., $r \in \{1\ 2\ \ldots\ n\}$, and $\boldsymbol{x} = (\{T_{ji}^{vf}\}\ \{\phi_i^f\}) = (x_1\ x_2 \ldots\ x_n)$ to be the solution vector. For the system of equations formed by (16b), (16c) and (23), $\mathcal{A}$ has full row rank and $\boldsymbol{b} = (0\ 0\ \ldots\ 0\ L)^T$. Therefore, there exists a unique solution to $(\{T_{ji}^{vf}\}\ \{\phi_i^f\})$. As per Farkas' lemma (Luenberger et al., 1984), exactly one of the feasible sets $\{\boldsymbol{x} \in \mathbb{R}^n | \mathcal{A}\boldsymbol{x} = \boldsymbol{b}\ \boldsymbol{x} \geq 0\}$ and $\{\boldsymbol{y} \in \mathbb{R}^n | \mathcal{A}^T\boldsymbol{y} \geq 0\ \ y_n < 0\}$ is non-empty. To prove that the latter set is empty, we drop Eq. (23) and consider the following primal and dual problems:

$$\text{(Primal problem)} \quad \max_{\boldsymbol{x}} \quad \boldsymbol{\delta}^T\boldsymbol{x} \tag{24a}$$

$$\text{s.t.} \quad \mathcal{A}_s\boldsymbol{x} = 0 \tag{24b}$$

$$\boldsymbol{x} \geq 0. \tag{24c}$$

$$\text{(Dual problem)} \quad \min_{\boldsymbol{y}^s} \quad \boldsymbol{0}^T\boldsymbol{y}_s \tag{25a}$$

$$\text{s.t.} \quad \mathcal{A}_s^T\boldsymbol{y}_s \geq \boldsymbol{\delta}. \tag{25b}$$

where $\boldsymbol{\delta} = (\delta_1\ \ldots\ \delta_n)$ is an n-dimensional vector satisfying $\boldsymbol{\delta} \geq 0$ and $\delta_n > 0$; $\boldsymbol{y}_s = (y_1\ y_2\ \ldots y_{n-1})$ is the vector formed by dual variables; $\mathcal{A}_s = (\boldsymbol{a}_1\ \ldots\ \boldsymbol{a}_n)$ is the $(n-1) \times n$-dimensional coefficient matrix for $\boldsymbol{x}$ formed by (16b) and (16c) after dropping one redundant equation from (16c). Notice that matrix $\mathcal{A}_s$ can be further expressed as a block matrix $\mathcal{A}_s = \begin{bmatrix} & \mathcal{A}_s^{12} \\ \mathcal{A}_s^{21} & \mathcal{A}_s^{22} \end{bmatrix}$ with being an $(|J|\ \ |I|) \times (|J|\ \ |I|)$ identical matrix, matrices $\mathcal{A}_s^{12}$ and $\mathcal{A}_s^{22}$ being the coefficient matrices for $\{\phi_i^f\}$ in Eqs. (16b) and (16c), respectively, matrix $\mathcal{A}_s^{21}$ being the coefficient matrix for $\{T_{ji}^{vf}\}$ in Eq. (16c).

By the construction of the above primal and dual problems, $y_n < 0$ holds only if both the primal problem (24) and dual problem (25) are feasible. However, problem (24) is unbounded and we reach a contradiction. One can check this observation

by replacing $\boldsymbol{x}$ with a vector $\boldsymbol{z}$ so that $\boldsymbol{x} = \mathcal{L}\boldsymbol{z}$ where $\mathcal{L}$ is a $n \times n$ square matrix given by $\mathcal{L} = \begin{bmatrix} & & -\mathcal{A}_s^{12} \\ & \boldsymbol{0} & \end{bmatrix}$. With this, the primal problem (24) is transformed into finding $\boldsymbol{z} \geq \boldsymbol{0}$ to satisfy $\mathcal{A}_s\mathcal{L}\boldsymbol{z} = \begin{bmatrix} & \boldsymbol{0} \\ \mathcal{A}_s^{21} & -\mathcal{M} \end{bmatrix} (z_1\ z_2\ \dots\ z_{n-1}) + \boldsymbol{c}_s\ \ z_n = 0$, where the vector $\boldsymbol{c}_s = (0\ 0\ \dots\ c_1\ c_2\ \dots\ c_{|I|-1}) \in \mathbb{R}^{n-1}$ with c_i equal to $\sum_{j:(m=|I|\ j)} Q_{mj} Pr_{i/j}$. $\mathcal{M}$ is a $(|I|-1)\times(|I|-1)$-dimensional matrix formed by the first $(n-1)$th columns of the matrix $(\mathcal{A}_s^{21}\mathcal{A}_s^{12} - \mathcal{A}_s^{22})$. The above system of linear equations has one degree of freedom. Given $z_n > 0$, the solution of $(z_1\ z_2\ \dots\ z_{n-1})$ can be calculated as $(z_1\ z_2\ \dots\ z_{|J|\ |I|}) = \boldsymbol{0}$ and $(z_{|J|\ |I|+1}\ \dots\ z_{n-1}) = -z_n\ \ \mathcal{M}^{-1}\boldsymbol{c}_s$. Note that matrix $\mathcal{M}$ is a M-matrix and $c_i > 0$, we have $\boldsymbol{z} \geq 0$ for a given $z_n > 0$. Plugging the solution $\boldsymbol{z}$ into $\mathcal{L}\boldsymbol{z}$ leads to a feasible solution to problem (24) that satisfies $x_n > 0$ and $\boldsymbol{\delta}^T\boldsymbol{x} > 0$. Because the value of z_n can be arbitrarily chosen over the interval $[0\ \infty)$, the problem (24) has unbounded solutions. By duality, the problem (25) is infeasible and the set $\{\boldsymbol{x} \in \mathbb{R}^n | \mathcal{A}\boldsymbol{x} = \boldsymbol{b}\ \boldsymbol{x} \geq 0\}$ must be non-empty.

(Condition A) We then prove by contradiction that the solution $\boldsymbol{x}$ is strictly positive. Assume there exists a zone $m \in I$ such that $\phi_m^f = 0$. This implies that $T_{jm}^{vf} = 0$ holds for all $j \in J$ by Eq. (16c). Because $\{Pr_{i/j}\}$ and $\{Q_{ij}^f\}$ are positively valued, the condition $T_{jm}^{vf} = 0$ suggests that $\phi_i^f = 0\ \forall i \in I$ and $T_{ji}^f = 0\ \forall j \in J\ \ i \in I$ hold following Eqs. (16b) and (16c). However, such a solution violates (23) and reaches a contradiction.

(Condition B) Note that $\{\{\varrho T_{ji}^{vf(L)}\}\ \{\varrho\phi_i^{f(L)}\}\}$ satisfy Eqs. (16b) and (16c) automatically for any arbitrary parameter $\varrho > 0$ given that L renders a solution $(\{T_{ji}^{vf(L)}\}\ \{\phi_i^{f(L)}\})$. Plugging $\{\{\varrho T_{ji}^{vf(L)}\}\ \{\varrho\phi_i^{f(L)}\}\}$ into the left-hand-side of (23) will equal ϱL. Because the solution to the above system of equations is unique, we must have $(\{T_{ji}^{vf(\varrho L)}\}\ \{\phi_i^{f(\varrho L)}\}) = (\{\varrho T_{ji}^{vf(L)}\}\ \{\varrho\phi_i^{f(L)}\})$, i.e., the solution $(\{T_{ji}^{vf(L)}\}\ \{\phi_i^{f(L)}\})$ homogeneously and linearly increases with the value of L. □

Step 3. We define a mapping $\boldsymbol{\Phi} : (\boldsymbol{N}^{vc}\ \boldsymbol{N}^{vf}) \rightrightarrows (\boldsymbol{N}^{vc}\ \boldsymbol{N}^{vf})$. Given $(\boldsymbol{N}^{vc}\ \boldsymbol{N}^{vf})$, $\boldsymbol{\Phi}$ first calculates parameters $\{w_i^p\}$, $\{Q_{ij}^k\}$, $\{w_i^{vk}\}$ and $\{Pr_{ji}\}$ following Eqs. (3), (6c), (10), (11), and (12). Then, it solves optimization (15) and (16) for updating $(\boldsymbol{N}^{vc}\ \boldsymbol{N}^{vf})$. Proposition 1 characterizes the continuity property of mapping $\boldsymbol{\Phi}$ regarding its inputs.

To prove this result of Proposition 1, we need the following results from literature.

Definition 1 (*Mangasarian-Fromovitz Constraint Qualification - MFCQ, Solodov et al. 2010*)**.** Consider a set $\boldsymbol{X}$ defined by a finite number of equality constraints $e_i(\boldsymbol{x}) = 0$ with $i \in \mathcal{I} = \{1\ 2\ 3\ ..\}$ and inequality constraints $g_j(\boldsymbol{x}) \leq 0$ with $j \in \mathcal{J} = \{1\ 2\ 3\ ..\}$, i.e., $\boldsymbol{X} = \{\boldsymbol{x} \in \mathbb{R}^n | e_i(\boldsymbol{x}) = 0\ \ i \in \mathcal{I}\ \ \ g_j(\boldsymbol{x}) \leq 0\ \ j \in \mathcal{J}\}$. Let $e_i(\boldsymbol{x}) : \mathbb{R}^n \to R$ and $g_j(\boldsymbol{x}) : \mathbb{R}^n \to R$ be continuously differentiable functions. At a feasible point $\hat{\boldsymbol{x}} \in \boldsymbol{X}$, let $A(\hat{\boldsymbol{x}})$ be the set of index j satisfying $g_j(\hat{\boldsymbol{x}}) = 0$, i.e., $A(\hat{\boldsymbol{x}}) = \{j \in \mathcal{J} | g_j(\hat{\boldsymbol{x}}) = 0\}$. MFCQ holds at $\hat{\boldsymbol{x}}$ if the following two conditions are satisfied:

1. $\{e_i'(\hat{\boldsymbol{x}})\ \forall i \in \mathcal{I}\}$ are linearly independent;
2. $\exists \boldsymbol{d} \in \mathbb{R}^n$ such that $\langle e_i'(\hat{\boldsymbol{x}})\ \boldsymbol{d}\rangle = 0\ \forall i \in \mathcal{I}$ and $\langle g_j'(\hat{\boldsymbol{x}})\ \boldsymbol{d}\rangle < 0\ \forall j \in A(\hat{\boldsymbol{x}})$.

where $e_i'(\boldsymbol{x})$ and $g_j'(\boldsymbol{x})$ denote the first derivatives of function $e_i(\boldsymbol{x})$ and $g_j(\boldsymbol{x})$ regarding $\boldsymbol{x}$, respectively; and $\langle\ \ \rangle$ means vector multiplication.

Definition 2 (*Slater Constraint Qualification, Solodov et al. 2010*)**.** Consider a set $\boldsymbol{X}$ as being defined in Definition 1. Slater constraint qualification assumes that the following conditions are satisfied:

1. $e_i(\boldsymbol{x})$ defines an affine function $\forall i \in \mathcal{I}$, and $g_j(\boldsymbol{x})$ is a convex function $\forall j \in \mathcal{J}$.
2. $\exists \hat{\boldsymbol{x}} \in \boldsymbol{X}$ such that $e_i(\hat{\boldsymbol{x}}) = 0\ \forall i \in \mathcal{I}$ and $g_j(\hat{\boldsymbol{x}}) < 0\ \forall j \in \mathcal{J}$.

Definition 3 (*Feasible Path Transfer Lower Semicontinuity-FTP Lower Semicontinuity Tian and Zhou, 1992*)**.** Let $\boldsymbol{X}$ and $\mathcal{Z}$ be two topological spaces and Γ: $\mathcal{Z} \to 2^X$ be a correspondence. The function $\pi : X \times \mathcal{Z} \to \mathbb{R}$ is FTP lower semicontinuity in ζ with respect to Γ if for each $(\boldsymbol{x}\ \zeta) \in X \times \mathcal{Z}$ with $\boldsymbol{x} \in \Gamma(\zeta)$ and $\forall\varepsilon > 0$, there exists some neighborhood $\mathcal{N}(\zeta)$ of ζ such that $\forall\overline{\zeta} \in \mathcal{N}(\zeta)$, $\exists$ (a feasible path) $\overline{\boldsymbol{x}} \in \Gamma(\overline{\zeta})$ satisfying $\pi(\boldsymbol{x}\ \zeta) < \pi(\overline{\boldsymbol{x}}\ \overline{\zeta}) + \varepsilon$.

Lemma 3 (*Tian and Zhou, 1992*)**.** *Let X and $\mathcal{Z}$ be two topological spaces. If*

i) $\pi : X \times \mathcal{Z} \to \mathbb{R}$ is an upper semicontinuous real-valued function;
ii) $\Gamma : \mathcal{Z} \to 2^X$ is a nonempty compacted-valued and closed correspondence;
iii) $\pi(\boldsymbol{x}\ \zeta)$ is FTP lower semicontinuity in $\zeta \in \mathcal{Z}$ with respect to Γ;
iv) Γ is upper semi-continuous,

Then, the maximum correspondence $S : \mathcal{Z} \to 2^X$, which is defined as $S(\zeta) = \{\boldsymbol{x} \in \Gamma(\zeta) : \pi(\boldsymbol{x}\ \zeta) \geq \pi(\boldsymbol{y}\ \zeta)\ \forall \boldsymbol{y} \in \Gamma(\zeta)\}$ for each $\zeta \in \mathcal{Z}$, is nonempty compact-valued, closed and upper semi-continuous.

Lemma 4 (*Berge's Maximum Theorem Ausubel and Deneckere, 1993*)**.** *Let X and $\mathcal{Z}$ be metric spaces, Γ: $\mathcal{Z} \rightrightarrows X$ be a compact-valued and non-empty correspondence, and $f : X \times \mathcal{Z} \to \mathbb{R}$ be a continuous function. If Γ is continuous, then $f^*(\zeta) = \max_{\boldsymbol{x}\in\Gamma(\zeta)} f(\boldsymbol{x}\ \zeta)$ is continuous at $\zeta \in \mathcal{Z}$ and $\boldsymbol{x}^* = \operatorname{argmax}_{\boldsymbol{x}\in\Gamma(\zeta)} f(\boldsymbol{x}\ \zeta)$ is upper semicontinuous, compact-valued and non-empty.*

Using these definitions and lemma, Proposition 1 is formally introduced as follows:

Proposition 1. *The mapping* $\Phi : (\boldsymbol{N^{vc}}\ \boldsymbol{N^{vf}}) \rightrightarrows (\boldsymbol{N^{vc}}\ \boldsymbol{N^{vf}})$ *is upper semicontinuous regarding its inputs* $\boldsymbol{N^{vc}} \geq \boldsymbol{0}$ *and* $\boldsymbol{N^{vf}} > \boldsymbol{0}$.

Proof. As defined, $\Phi(\boldsymbol{N^{vc}}\ \boldsymbol{N^{vf}})$ involves solving optimization problems (15) and (16) for contractors and freelancers, respectively. To this end, we define two mappings $\mathcal{S}^c$ and $\mathcal{S}^f$ that map the inputs parameters $\zeta^c \in \mathcal{Z}^c$ and $\zeta^f \in \mathcal{Z}^f$ of problems (15) and (16) to their corresponding optimal solutions $\boldsymbol{N^{vc}}$ (ζ^c) and $\boldsymbol{N^{vf}}$ (ζ^f), respectively:

$$\mathcal{S}^c : \mathcal{Z}^c \rightrightarrows \{\boldsymbol{N^{vc}}\ (\zeta^c) \in \Gamma^c(\zeta^c) | \boldsymbol{N^{vc}} \in \underset{\{\boldsymbol{N^{vc}}\ T^{vc}_{ji}\ \phi^c_i\}}{\operatorname{argmax}} \pi^c(\boldsymbol{N^{vc}}\ T^{vc}_{ji} | \zeta^c) \quad \text{where } \zeta^c \in \mathcal{Z}^c\} \tag{26}$$

$$\mathcal{S}^f : \mathcal{Z}^f \rightrightarrows \{\boldsymbol{N^{vf}}\ (\zeta^f) \in \Gamma^f(\zeta^f) | \boldsymbol{N^{vf}} \in \underset{\{\boldsymbol{N^{vf}}\ T^{vf}_{ji}\ \phi^f_i\ \delta^f_i\}}{\operatorname{argmax}} \pi^f(\phi^f_i\ \delta^f_i | \zeta^f) \quad \text{where } \zeta^f \in \mathcal{Z}^f\}. \tag{27}$$

Here, $\mathcal{Z}^k$ denotes the set associated with parameters ζ^k for each driver type $k \in \{f\ c\}$; $\Gamma^c(\zeta^c)$ and $\Gamma^f(\zeta^f)$ denote the feasible set of problems (15) and (16) for given parameters ζ^c and ζ^f, respectively. For contractors, parameter ζ^c is characterized by a tuple $(\{w^p_i\}\ Q^c_{ij}\ w^{vc}_i\})$, where additional information on freelancers' cruising probability $\{Pr_{i/j}\}$ is necessary for solving (16) and $\zeta^f = (\{w^p_i\}\ \{Q^f_{ij}\}\ \{w^{vf}_i\}\ \{Pr_{i/j}\})$.

Given $\boldsymbol{N^{vc}} \geq \boldsymbol{0}$ and $\boldsymbol{N^{vf}} > \boldsymbol{0}$, trip demand $\{Q^k_{ij}\}$ and customers' waiting time $\{w^p_i\}$ can be uniquely determined by (10) and (11). Since both $f_w(\,)$ and $f(\,)$ prescribe continuous functions, $\{w^p_i\}$ and $\{Q^k_{ij}\}$ change continuously with $(\boldsymbol{N^{vc}}\ \boldsymbol{N^{vf}})$. By Eq. (12), drivers' average waiting time $\{w^{vk}_i\}$ is also continuous with respect to $(\boldsymbol{N^{vc}}\ \boldsymbol{N^{vf}})$. Because $Q_{ij} > 0$ for all OD pair $(i\ j) \in W$ (Condition C.2 and C.3), freelancers' utility $\{U_{ji}\}$ are well defined and continuous regarding $\{Q_{ij}\}$ and $\{w^{vf}_i\}$. Therefore, their cruising probability $\{Pr_{i/j}\}$ are continuous with $(\boldsymbol{N^{vc}}\ \boldsymbol{N^{vf}})$ following Eqs. (3) and (6c). The above indicates that the parameter ζ^k continuously changes with $(\boldsymbol{N^{vc}}\ \boldsymbol{N^{vf}})$. Therefore, proving Proposition 1 is equivalent to proving that the mapping $\mathcal{S}^k(\zeta^k)$ is upper semicontinuous regarding $\zeta^k \in \mathcal{Z}^k$ for $k \in \{f\ c\}$. The following Lemma 5 provides such a result regarding the continuity of $\mathcal{S}^k$, which completes the proof of this proposition. □

We invoke the following lemma to prove the upper semicontinuity of $\mathcal{S}^k(\zeta^k)$:

Lemma 5. *Mapping* $\mathcal{S}^k$, *as defined in* (26) *and* (27), *is upper semicontinuous regarding* $\zeta^k \in \mathcal{Z}^k$ *for* $k \in \{f\ c\}$.

Proof. We apply Berge's maximum theorem (see Lemma 4) to prove Lemma 5. We first define two mappings Γ^k $(k \in \{f\ c\})$ that maps from the parameter space $\mathcal{Z}^k$ formed by inputs ζ^k to the corresponding feasible sets of (15) and (16), respectively. For contractors, the mapping Γ^c takes $\zeta^c = (\{Q^c_{ij}\}\ \{w^p_i\}\ \{w^{vc}_i\})$ as inputs:

$$\Gamma^c : \mathcal{Z}^c \rightrightarrows \boldsymbol{X} : \{\boldsymbol{x} = \{T^{vc}_{ji}\ \phi^c_i\ N^{vc}_i\} | (15b)\text{–}(15f)\ \phi^c_i \geq 0\ T^{vc}_{ji} \geq 0\}.$$

For given input ζ^c, the feasible set $\Gamma^c(\zeta^c)$ is non-empty since problem (15) warrants a feasible solution $N^{vc}_i = N^c/|I|$, $\phi^c_i = 0$ for $i \in I$ and $T^{vc}_{ji} = 0$ for $j \in J\ i \in I$. Since constraints (15b)–(15f) define a non-empty polyhedron, $\Gamma^c(\zeta^c)$ is closed-valued. Also, the feasible set $\Gamma^c(\zeta^c)$ is bounded (considering the modified fleet conservation condition (15d), the boundary condition (15f), and the non-negativity constraints for $\{T^{vc}_{ji}\}$ and $\{\phi^c_i\}$). Therefore, the mapping Γ^c essentially defines a compact-valued correspondence from the parameter space $\mathcal{Z}^c$ to the feasible set X.

For freelancers, the feasible set mapping Γ^f takes ζ^f as inputs and is defined as follows:

$$\Gamma^f : \mathcal{Z}^f \rightrightarrows \boldsymbol{Y} : \{\boldsymbol{y} = \{T^{vf}_{ji}\ \phi^f_i\ N^{vf}_i\ \delta^f_i\} | (16b)\text{–}(16f)\ \phi^f_i \geq 0\ T^{vf}_{ji} \geq 0\ \delta^f_i \geq 0\}.$$

Here, in addition to $\{Q^f_{ij}\}$, $\{w^p_i\}$ and $\{w^{vf}_i\}$, parameter $\boldsymbol{\zeta^f} \in \mathcal{Z}^f$ contains additional information on freelancers' cruising probability $\{Pr_{i/j}\}$, i.e., $\zeta^f = (\{Q^f_{ij}\}\ \{w^p_i\}\ \{w^{vf}_i\}\ \{Pr_{i/j}\})$. For a given input ζ^f, the feasible set $\Gamma^f(\zeta^f)$ is non-empty since problem (16) warrants a feasible solution $N^{vf}_i = \delta^f_i = N^f/|I|$, $\phi^f_i = 0$ for $i \in I$ and $T^{vf}_{ji} = 0$ for $j \in J\ i \in I$. Also, Γ^f is compacted-valued.

Note that both the objective functions of (15) and (16) are continuous. Therefore, Lemma 4 suggests that mapping $\mathcal{S}^k(\zeta^k)$ is upper semicontinuous if Γ^k is continuous. To this end, the following characterize the continuity properties (upper and lower semicontinuity) of the mapping Γ^k and proves the upper semicontinuity $\mathcal{S}^k$ for contractors and freelancers, respectively.

a) Upper semicontinuity of $\mathcal{S}^c(\zeta^c)$. We first show that mapping Γ^c is upper semi-continuous. Since the feasible set $\Gamma^c(\zeta^c)$ is a non-empty and bounded polyhedron, mapping Γ^c is upper-Lipschitz-continuous (Robinson, 1977), i.e., there exists a constant $l > 0$ such that the condition $\Gamma^c(\zeta^{c'}) \subset \{\boldsymbol{x} | dis(\boldsymbol{x}\ \Gamma^c(\zeta^c)) \leq l\ \|\zeta^c - \zeta^{c'}\|\}$ holds for $\zeta^{c'} \in B_\varepsilon(\zeta^c)$. Here, $dis(\boldsymbol{x}\ \Gamma^c) = \inf\{\|\boldsymbol{x} - \boldsymbol{x}'\| \ |\boldsymbol{x}' \in \Gamma^c(\zeta^c)\}$. Hence, Γ^c is upper semicontinuous (Davidson, 1996).

Next, we discuss the lower semicontinuity of mapping Γ^c if

1. $Q^c_{ij} > 0$ for all $(i\ j) \in W$;
2. $\exists m \in I$ such that $Q^c_{mj} = 0$ holds for any $(m\ j) \in W$.

In the first case where $Q^c_{ij} > 0$ for all $(i\ j) \in W$, proving the lower semi-continuity of Γ^c can reduce to prove that MFCQ (see Definition 1) holds at any $\boldsymbol{x} \in \Gamma^c(\zeta^c)$ (Robinson, 1977; Davidson, 1996; Still, 2018). Note that the rows of the coefficient matrix defined by constraints (15b) and (15c) are linearly dependent since $\sum_{i\in I}\sum_{j:(i\ j)\in W} Q^c_{ij}\ \phi^c_i = \sum_{j\in J}\sum_{i:(i\ j)\in W} Q^c_{ij}\ \phi^c_i$. Therefore, one can eliminate one redundant constraint so that the feasible region remains the same. Let H and G denote the resultant coefficient matrix formed by equality constraints and inequality constraints of problem (15), respectively. Then, the feasible set can be denoted

as $\{\boldsymbol{x}|H\boldsymbol{x}=\mathbf{0}\ G\boldsymbol{x}\le 0\}$, and H has full row rank. With this, proving that MFCQ holds is equivalent to proving the satisfaction of Slater CQ (see Definition 2) which means that there exists a feasible solution $\hat{\boldsymbol{x}}$ satisfying $H\hat{\boldsymbol{x}}=\mathbf{0}$ and $G\hat{\boldsymbol{x}}<0$ (Davidson, 1996; Solodov et al., 2010).

Consider $\hat{\boldsymbol{x}}=(\{\widehat{\phi}_i^f\}\ \{\widehat{T}_{ji}^{vf}\}\ \{\widehat{N}_i^{vf}\})$ that consists of the following components:

$$\widehat{\phi_i^c}=\sigma \quad \forall i\in I \tag{28}$$

$$\widehat{T_{ji}^{vc}}=\sigma\ \Big(\sum_{m:(m\,j)\in W} Q_{mj}^c\Big)\ \frac{\sum_{d:(i\,d)\in W} Q_{id}^c}{\sum_{(m\,d)\in W} Q_{md}^c} \quad \forall j\in J\ i\in I \tag{29}$$

$$\widehat{N_i^{vc}}=\sum_{j\in J}\widehat{T_{ji}^{vc}}\ w_i^{vc}+\Delta^c \quad \forall i\in I \tag{30}$$

where $\sigma>0$ and $\Delta^c>0$. With the above solution, $\hat{\boldsymbol{x}}$ satisfies constraints (15b) and (15c). Plugging $\hat{\boldsymbol{x}}$ into (15d) leads to the following equation:

$$\sigma\ \ \psi(Q_{ij}^c\ w_i^p\ w_i^{vc}\ h_{ij}\ h_{ji})+|I|\ \ \Delta^c=N^c. \tag{31}$$

where $\psi(Q_{ij}^c\ w_i^p\ w_i^{vc}\ h_{ij}\ h_{ji})$ is prescribed as follows:

$$\psi(Q_{ij}^c\ w_i^p\ w_i^{vc}\ h_{ij}\ h_{ji})=\sum_{(i\,j)\in W} Q_{ij}^c\ (h_{ij}+w_i^p)+\sum_{j\in J}\sum_{i\in I}\left(\sum_{m:(m\,j)\in W} Q_{mj}^c\ \frac{\sum_{d:(i\,d)\in W} Q_{id}^c}{\sum_{(m\,d)\in W} Q_{md}^c}\right)\ (h_{ji}+w_i^{vc}). \tag{32}$$

Because $Q_{ij}^c>0$ for all $(i\ j)\in W$, $\psi>0$ holds for given ζ^c. With this, it suffices to show that there exists $\sigma\in(0\ \ M_2^c)$ and $\Delta^c>0$ such that (31) holds as follows:

$$\begin{cases}\sigma=1\ \ \Delta^c=\frac{N^c-\psi}{|I|} & \text{if } \psi(Q_{ij}^c\ w_i^p\ w_i^{vc}\ h_{ij}\ h_{ji})<N^c;\\ \sigma=\frac{N^c}{\psi}\ \ \frac{1}{|I|+1}\ \ \Delta^c=\frac{N^c}{|I|+1} & \text{Otherwise.}\end{cases} \tag{33}$$

With σ and Δ^c prescribed in (28) and (33)–(30), $\hat{\boldsymbol{x}}$ satisfies $H\hat{\boldsymbol{x}}=\mathbf{0}$ and $G\hat{\boldsymbol{x}}<0$. Therefore, the Slater CQ holds, and $\Gamma^c(\zeta^c)$ is lower semi-continuous at ζ^c when $Q_{ij}^c>0$ for all $(i\ j)\in W$.

For the second case where there exists a zone $m\in I$ such that $Q_{mj}^c=0$, MFCQ does not hold since $\sum_{j:(m\,j)\in W} Q_{mj}$ equals 0 and no idle contractors flow into zone m, i.e., $T_{jm}^{vc}=0$ for any $j\in J$. To prove the upper semicontinuity of $S^c(\boldsymbol{\zeta}^c)$, we apply a weakened condition called "feasible path transfer semicontinuity" (FTP), as stated in Definition 3 and Lemma 3. To apply Lemma 3, we note that function π in Lemma 3 corresponds to objective function (15a), and Γ and ζ correspond to Γ^c and $\boldsymbol{\zeta}^c$, respectively. For Problem (15), condition (i) in Definition 3 holds because the objective (15a) prescribes a single-valued continuous function. Recall that Γ^c is compacted-valued and upper semicontinuous, condition (ii) and (iv) also hold. To prove condition (iii), let $\varepsilon>0$ and consider the neighborhood $\mathcal{N}(\zeta^c)=\{\bar{\zeta}^c|\ \|\zeta^c-\zeta^c\|_2\le\varepsilon\ \bar{Q}_{mj}^c>0\ \ \|\bar{\zeta}^c-\zeta^c\|_2=\sqrt{\sum_{j:(m\,j)\in W}(\bar{Q}_{mj}^c)^2}\}$ for a given ζ^c that have components $Q_{mj}^c=0$, $m\in I$ and $(m\ j)\in W$. More specifically, ζ^c and $\hat{\zeta}^c$ only differs in the values of components $\{Q_{mj}^c\}_{(m\,j)\in W}$. Then, given ζ^c, the set $\{\pi(\boldsymbol{x}(\zeta^c)\ \zeta^c)|\boldsymbol{x}\in\Gamma^c(\boldsymbol{\zeta}^c)\}$ that is formed by the objective function values of (15a) can be retained at $\bar{\zeta}^c$ by setting $\bar{\phi}_m^c=0$ for any $\bar{\zeta}^c\in\mathcal{N}(\boldsymbol{\zeta}^c)$, leading to the condition $\{\pi(\boldsymbol{x}\ \zeta^c)|\boldsymbol{x}\in\Gamma^c(\zeta^c)\}\subset\{\pi(\bar{\boldsymbol{x}}\ \bar{\zeta}^c)|\bar{\boldsymbol{x}}\in\Gamma^c(\bar{\zeta}^c)\}$. Therefore, condition (iii) holds and $S^c(\zeta^c)$ is upper semicontinuous at ζ^c.

b) Upper semicontinuity of $S^f(\zeta^f)$. We prove the upper semicontinuity of $S^f(\zeta^f)$ by proving that the feasible set mapping Γ^f is continuous. **b1)** Note that the feasible set $\Gamma^f(\zeta^f)$ is a non-empty, closed and bounded polytope. Therefore, $\Gamma^f(\zeta^f)$ features upper Lipschitz continuity at ζ^f, implying the upper semicontinuity of $\Gamma^f(\zeta^f)$ at ζ^f. **b2)** Mapping Γ^f is lower semi-continuous regarding its inputs because MFCQ holds for feasible solutions $\boldsymbol{y}\in\Gamma^f(\zeta^f)$. Given $\boldsymbol{N^{vf}}>\mathbf{0}$, Eq. (10) suggests that the trip demand for freelancers Q_{ij}^f satisfies $Q_{ij}^f>0$ for any OD pair $(i\ j)\in W$. We can drop one equation from (16c) and the remaining equations are linearly independent. Then, proving the satisfaction of MFCQ for any $\boldsymbol{y}\in\Gamma^f(\zeta^f)$ is equivalent to proving that Slater CQ holds for problem (16). Consider a solution $\hat{\boldsymbol{y}}$ that have components $\hat{\delta}_i^f=\Delta^f$ and $\widehat{N}_i^{vf}=\sum_{j\in J}\widehat{T}_{ji}^{vf}w_i^{vf}+\Delta^f\ \forall i\in I$ where Δ^f is a constant and satisfies $\Delta^f\in[\xi\ \ \frac{N^f}{|I|})$. Plugging $\hat{N}_i^{vf}$ into problem (16) transforms constraint (16d) into the following equation:

$$\sum_{(i\,j)\in W} Q_{ij}^f\hat{\phi}_i^f\ \ (h_{ij}+w_i^p)+\sum_{j\in J}\sum_{i\in I}\widehat{T}_{ji}^{vf}\ \ (h_{ji}+w_i^{vf})=N^f-|I|\Delta^f. \tag{34}$$

Note that $N^f-|I|\Delta^f>0$ holds, as per Lemma 2, there exists unique solution $\hat{\phi}_i^f>0$ and $\widehat{T}_{ji}^{vf}>0$ satisfying (16b), (16c) and (16d) for any fixed $\Delta^f\in[\xi\ \ \frac{N^f}{|I|})$. This further leads to $\widehat{N}_i^{vf}>\xi\ \forall i\in I$ and constraint (16f) is satisfied. Also, Eqs. (16b), (16c) and (16d) are satisfied with the solution $\hat{\phi}_i^f>0$, $N_i^{vf}>\xi$, $N_i^{vf}>\sum_j\widehat{T}_{ji}^{vf}\ \ \widehat{w}_i^{vf}$, $T_{ji}^{vf}>0$ and $\delta_i^f>0$. Therefore, Slater CQ holds and mapping Γ^f is lower semi-continuous.

The upper and lower semicontinuity of $\Gamma^f(\zeta^f)$ indicate that $\Gamma^f(\zeta^f)$ is continuous at ζ^f. Applying Berge's maximum theorem in Lemma 4, we prove the upper semicontinuity of S^f. □

B.2. Proof of Theorem 1

Proof. We prove Theorem 1 in two steps. First, we prove the existence of fixed points with the defined mapping $\Phi(\boldsymbol{N^{vc}}\ \boldsymbol{N^{vc}})$ by Kakutani's fixed point theorem. Second, we show that the derived fixed point satisfies the equilibrium condition defined by (14).

B.2.1. Proof for the existence of fixed point

According to Kakutani's fixed point theorem (Granas and Dugundji, 2003), a set-valued map $\phi : \mathcal{Z} \to 2^{\mathcal{Z}}$ ensures a fixed point if: (i) $\mathcal{Z}$ is non-empty, compact and convex: (ii) $\phi(z)$ is non-empty and convex for all $z \in \mathcal{Z}$; (iii) ϕ has a closed graph.

In our setting, $\boldsymbol{\Phi}(\boldsymbol{N^{vc}}\ \boldsymbol{N^{vf}})$ defines a set-valued mapping from Ω to 2^{Ω}, i.e., $\boldsymbol{\Phi} : \Omega \to 2^{\Omega}$, where 2^{Ω} denotes the set of all subsets of Ω. We define a space $\Omega = \{(\boldsymbol{N^{vc}}\ \boldsymbol{N^{vf}}) | N_i^{vc} \in [0\ N^c]\ N_i^{vf} \in [\xi\ N^f]\}$ where the bound $\xi > 0$ is derived in Lemma 1. Given $(\boldsymbol{N^{vc}}\ \boldsymbol{N^{vf}}) \in \Omega$, mapping $\boldsymbol{\Phi}$ first updates the market status ζ characterized by customers' average waiting time $\{w_i^p\}$, the trip demand $\{Q_{ij}^k\}$, and drivers' average waiting time following Eqs. (10), (11), and (12). Additional information on freelancers' routing probability is determined following Eqs. (3) and (6c) with $Pr_{i/j} \in (0\ 1)\ \forall j \in J\ i \in I$. Finally, with ζ^c as input parameters, solving optimization problem (15) lead to $N_i^{vc*}(\zeta^c) \in [0\ N^c]$ for $i \in I$ considering constraints (15d) and (15e) and the non-negative constraints for variables $\{T_{ji}^{vc}\}$ and $\{\phi_i^c\}$. Given input $\zeta^f = (\{w_i^p\}\ \{Q_{ij}^f\}\ \{w_i^{vf}\}\ \{Pr_{i/j}\})$, solving optimization problem (16) gives the solution $N_i^{vf*}(\zeta^f) \in [\xi\ N^f]\ \forall i \in I$ considering constraints (16d), (16f) and the non-negative constraints for variables $\{T_{ji}^{vf}\}$, $\{\phi_i^f\}$ and $\{\delta_i^f\}$.

Condition i) By our definition of Ω, i.e., $\Omega = \{(\boldsymbol{N^{vc}}\ \boldsymbol{N^{vf}}) | N_i^{vc} \in [0\ N^c]\ N_i^{vf} \in [\xi\ N^f]\}$, condition (i) is satisfied because $\xi < N^f$ and Ω is compact and convex.

Condition ii) $\boldsymbol{\Phi}(\boldsymbol{N^{vc}}\ \boldsymbol{N^{vf}})$ is non-empty and convex because: First, for given $(\boldsymbol{N^{vc}}\ \boldsymbol{N^{vf}}) \in \Omega$, the inputs ζ^c and ζ^f for contractors' and freelancers' optimization problems (15) and (16) are uniquely determined. Second, given ζ^c and ζ^f, two optimization problems (15) and (16) have feasible solutions, respectively (see Proposition 1). Therefore, the set $\boldsymbol{\Phi}(\boldsymbol{N^{vc}}\ \boldsymbol{N^{vf}})$ is nonempty. Third, Condition C.4 ensures that the first term of the objective (15a) is strictly concave regarding $\boldsymbol{N^{vc}}$. Consequently, the input ζ^c leads to a unique solution $\boldsymbol{N^{vc}}\ (\zeta^c)$ for problem (15). Given ζ^f, the optimal solution $\boldsymbol{N^{vf}}\ (\zeta^f)$ belongs to a convex set ((16) is a linear program). Therefore, given any $(\boldsymbol{N^{vc}}\ \boldsymbol{N^{vf}}) \in \Omega$, the set $\boldsymbol{\Phi}(\boldsymbol{N^{vc}}\ \boldsymbol{N^{vf}})$ is convex.

Condition iii) Theorem 17.11 in Guide (2006) showed that in a Hausdorff space Condition (iii) is satisfied if the mapping $\boldsymbol{\Phi}$ is (1) upper semicontinuous and (2) closed-valued. Property (1) is proved by Proposition 1. Property (2) holds since $\boldsymbol{N^{vc}}\ (\zeta^c)$ is unique given input ζ^c and the set of $\boldsymbol{N^{vf}}\ (\zeta^f)$ forms a polyhedron given inputs ζ^f. Therefore, given $(\boldsymbol{N^{vc}}\ \boldsymbol{N^{vf}}) \in \Omega$, the set $\boldsymbol{\Phi}(\boldsymbol{N^{vc}}\ \boldsymbol{N^{vf}})$ is closed valued.

Summarizing Conditions (i)–(iii), the mapping $\boldsymbol{\Phi}$ ensures a fixed point over Ω.

B.2.2. Verification of equilibrium conditions

This subsection shows that the fixed point satisfies the equilibrium conditions of (14) by further examining optimal solutions to (15) and (16). We use $\hat{x}$ and x^* to differentiate the input and the optimal solution of optimization problems, respectively.

1) Verification of MNE condition (14a). For contractors, proving that the fixed point satisfies the MNE condition (14a) is equivalent to proving that constraints (15e) are active at the fixed point and the optimality conditions of problem (15) at the fixed point replicates those of problem (13).

First, we prove constraints (15e) are active at the fixed point. When $\hat{N}_i^{vc} = 0$, we have $\sum_j T_{ji}^{vc*}(\zeta^c) = 0$ and $N_i^{vc*} = \sum_j T_{ji}^{vc*}(\zeta^c)\ \hat{w}_i^{vc}$. Therefore, constraints (15e) are active for zone i if $\hat{N}_i^{vc} = 0$. For the zones satisfying $\hat{N}_i^{vc} > 0$, we can reformulate constraints (15e) as $N_i^{vc} \geq \phi_i^c\ \hat{N}_i^{vc}\ \forall i \in I$ because $\sum_{j \in J} T_{ji}^{vc}\ \hat{w}_i^{vc} = \phi_i^c \sum_{j:(i\ j) \in W} \hat{Q}_{ij}^c\ \hat{w}_i^{vc}$, $\hat{w}_i^{vc} = \hat{N}_i^{vc} / \sum_{j:(i\ j) \in W} \hat{Q}_{ij}^c$ and $\sum_{j:(i\ j) \in W} \hat{Q}_{ij}^c > 0$. Since $\hat{N}_i^{vc} = N_i^{vc*}(\zeta^c)$ at the fixed point, the relation $N_i^{vc} \geq \phi_i^c\ \hat{N}_i^{vc}$ implies that $\phi_i^{c*}(\zeta^c) \in (0\ 1]$ given inputs $\hat{N}_i^{vc} > 0$. Therefore, constraint (15f) can be dropped from problem (15) at the fixed point, leading to the following KKT conditions:

$$T_{ji}^{vc*} \geq 0 \quad \forall j \in J\ i \in I \tag{35a}$$

$$(-M_1^c + \lambda_i)\ \hat{w}_i^{vc} + \mu_i + \mu_j + \nu\ h_{ji} \geq 0 \quad \forall j \in J\ i \in I \tag{35b}$$

$$T_{ji}^{vc*}\ \{(-M_1^c + \lambda_i)\ \hat{w}_i^{vc} + \mu_i + \mu_j + \nu\ h_{ji}\} = 0 \quad \forall j \in J\ i \in I \tag{35c}$$

$$-\sum_{j:(i\ j) \in W} F_{ij}\ \frac{\partial Q_{ij}}{\partial N_i^{vc}}|_{N_i^{vc*}} + \nu + M_1^c - \lambda_i = 0 \quad \forall i \in I \tag{35d}$$

$$\lambda_i\ (N_i^{vc*} - \sum_{j \in J} T_{ji}^{vc*}\ \hat{w}_i^{vc}) = 0 \quad \forall i \in I \tag{35e}$$

$$\lambda_i \geq 0 \quad \forall i \in I \tag{35f}$$

$$\nu \sum_{j:(i\ j) \in W} \hat{Q}_{ij}^c\ (h_{ij} + \hat{w}_i^p) - \sum_{j:(i\ j) \in W} \hat{Q}_{ij}^c\ (\mu_i + \mu_j) \geq 0 \quad \forall i \in I \tag{35g}$$

$$\phi_i^{c*} \left(\nu \sum_{j:(i\ j) \in W} \hat{Q}_{ij}^c\ (h_{ij} + \hat{w}_i^p) - \sum_{j:(i\ j) \in W} \hat{Q}_{ij}^c\ (\mu_i + \mu_j) \right) = 0 \quad \forall i \in I \tag{35h}$$

$$\phi_i^{c*} \geq 0 \quad \forall i \in I \tag{35i}$$

(15b), (15c), (15d), (15e)

where $\mu_i\ \mu_j\ \nu\ \lambda_i$ are the Lagrangian multipliers associated with constraints (15b)–(15e).

For a zone m with $\hat{N}_m^{vc} > 0$, we prove that constraints (15e) are active and $\phi_m^{c*}(\zeta^c) = 1$ at the fixed point by contradiction. Assuming that constraint (15e) is inactive and $\phi_m^{c*}(\zeta^c) < 1$ holds at the fixed point. In this case, Eq. (35e) suggests $\lambda_m = 0$, which implies $\nu < 0$ by Eq. (35d) because $M_1^c > \sum_{j:(m\,j)\in W} F_{mj} \quad \partial Q_{mj}/\partial N_m^{vc}$. With $\lambda_m = 0$ and $\nu < 0$, the inequality (35b) indicates that $\mu_m + \mu_j \geq 0$ holds for all $j \in J$, leading to $\sum_{j:(m\,j)\in W}(\mu_m + \mu_j) \geq 0$. However, this contradicts the inequality (35g).

Next, we show that the optimal solution to (15) at the fixed point satisfies the KKT conditions of (13). Since constraints (15e) are active at the fixed point, (15e) becomes equalities. By setting $\phi_i^{c*}(\zeta^c) = 1 \ \forall i \in I$ and removing (35h) and (35i), the remaining conditions are essentially KKT conditions for (13). Therefore, the derived fixed point satisfies the MNE condition (14a).

2) Verification of MNE condition (14b) and (14c). For freelancers, verifying that fixed point satisfies the MNE conditions (14b) and (14c) is equivalent to proving that problem (16) has optimal solutions $\delta_i^{f*}(\zeta^f) = 0$ and $\phi_i^{f*}(\zeta^f) = 1 \ \forall i \in I$ at the fixed point. Here, $\delta_i^{f*}(\zeta^f) = 0 \ \forall i \in I$ can be inferred by comparing constraints (16e) with (6f) while $\phi_i^{f*}(\zeta^f) = 1 \ \forall i \in I$ is derived according to (6b) and (16b).

For problem (16), notice that constraints (16e) can be reformulated as $N_i^{vf} = \delta_i^f + \phi_i^f \ \hat{N}_i^{vf} \ \forall i \in I$ in viewing that $\sum_{j\in J} T_{ji}^{vf} \ \hat{w}_i^{vf} = \phi_i^f \hat{w}_i^{vf} \ \sum_{j:(i\,j)\in W} \hat{Q}_{ij}^f$ and $\hat{w}_i^{vf} = \sum_{k\in\{f\,c\}} \hat{N}_i^{vk} / \sum_{k\in\{f\,c\}} \sum_{j:(i\,j)\in W} \hat{Q}_{ij}^k = \hat{N}_i^{vf} / \sum_{j:(i\,j)\in W} \hat{Q}_{ij}^f$ for any given input $\hat{N}_i^{vf} > 0$ and $i \in I$. Since $N_i^{vf*}(\zeta^f) = \hat{N}_i^{vf} \ \forall i \in I$ holds at the fixed point, the relation $N_i^{vf} = \delta_i^f + \phi_i^f \ \hat{N}_i^{vf}$ implies that problem (16) has optimal solutions $\phi_i^{f*} = 1$ if $\delta_i^{f*}(\zeta^f) = 0$, or $\phi_i^{f*} = 1 \in (0\ 1)$ if $\delta_i^{f*}(\zeta^f) > 0$. The following proves $\delta_i^{f*}(\zeta^f) = 0 \ \forall i \in I$ by showing that the second solution $\delta_i^{f*}(\zeta^f) > 0$ is not obtainable at the fixed point.

First, we prove by contradiction that $N_i^{vf*}(\zeta^f) = \xi$ holds if $\delta_i^{f*}(\zeta^f) > 0$ in the optimal solution to (16). Assuming that there exists a zone $m \in I$ such that $N_m^{vf*}(\zeta^f) > \xi$ and $\delta_m^{f*}(\zeta^f) > 0$. Then, Lemma 2 suggests that reducing the value of $\delta_m^{f*}(\zeta^f)$ by a small number will increase $\phi_i^{f*}(\zeta^f)$ for any $i \in I$. As the objective function (16a) increases with the value of ϕ_i^f and decreases with the value of δ_i^f, This feasible solution does not violate any constraint and obtains a higher objective function value, which contradicts the fact that $\phi_i^{f*}(\zeta^f)$ is the optimal solution.

Next, we prove that $N_i^{vf*}(\zeta^f) = \xi$ cannot be obtained at the fixed point by contradiction. Assume that there exists a zone $m \in I$ such that $N_m^{vf*}(\zeta^f) = \xi$ and $\delta_m^{f*}(\zeta^f) > 0$ hold at the fixed point. Now, given the same input $\zeta^f = (\{w_i^p\}\ \{Q_{ij}^f\}\ \{w_i^{vf}\}\ \{Pr_{i/j}\})$, we drop δ_i^f from (16e) and solve a system of linear equations formed by (16b), (16c) and the following formula:

$$\sum_{(i\,j)\in W} \hat{Q}_{ij}^f \phi_i^f \quad (h_{ij} + \hat{w}_i^p) + \sum_{j\in J}\sum_{i\in I} T_{ji}^{vf} \quad (h_{ji} + \hat{w}_i^{vf}) = N^f. \tag{36}$$

We denote the solution to the above system of equations as $\{\widetilde{\phi}_i^f\}$ and $\{\widetilde{T}_{ji}^{vf}\}$ for differentiation. Since $\delta_m^{f*}(\zeta^f) > 0$ at the fixed point, we have $N^f - \sum_{i\in I} \delta_i^{f*}(\zeta^f) < N^f$. Consequently, Lemma 2 suggests that $\phi_i^{f*}(\zeta^f) < \widetilde{\phi}_i^f(\zeta^f) \ \forall i \in I$ and $T_{ji}^{vf*}(\zeta^f) < \widetilde{T}_{ji}^{vf}(\zeta^f) \ \forall j \in J \ i \in I$ hold. Recall that the solutions to problem (16) satisfy $N_i^{vf} = \delta_i^f + \phi_i^f \ \hat{N}_i^{vf} \ \forall i \in I$. Therefore, given the same ζ^f, we have $N_i^{vf*}(\zeta^f) < \widetilde{N}_i^{vf}(\zeta^f)$ for zone $i \in I$ and $i \quad m$ and $N_m^{vf*}(\zeta^f) > \widetilde{N}_m^{vf}(\zeta^f)$ for zone m. Since $N_m^{vf*}(\zeta^f) = \xi$ by assumption, we have $\widetilde{N}_m^{vf}(\zeta^f) < \xi$ for m. Because $N_m^{vf*} = \hat{N}_m^{vf}$ hold at the fixed point and $\widetilde{N}_m^{vf}(\zeta^f) = \widetilde{\phi}_i^f \hat{N}_m^{vf} \ \forall i \in I$, the fact $\widetilde{N}_m^{vf}(\zeta^f) < \xi$ and $N_m^{vf*} = \xi$ imply $\widetilde{\phi}_m^f < 1$ for m. Also, for Eqs. (16b), (16c) and (36) to be satisfied, we have the following inequalities:

$$N^f = \sum_{(i\,j)\in W} \hat{Q}_{ij}^f \widetilde{\phi}_i^f \quad (h_{ij} + \hat{w}_i^p) + \sum_{j\in J}\sum_{i\in I} \widetilde{T}_{ji}^{vf} \quad (h_{ji} + \hat{w}_i^{vf}) \leq \sum_{(i\,j)\in W} \hat{Q}_{ij}^f \widetilde{\phi}_i^f \quad \left(2\overline{h} + \overline{w}_i^p + \overline{w}_i^{vf}\right)$$

where $\overline{h} = \max_{i\in I\ j\in J}\{h_{ij}\ h_{ji}\}$; $\overline{w}_i^p$ and $\overline{w}_i^{vf}$ denotes the common upper bounds for the average waiting time of customers and freelancers, respectively, which exist given inputs $\hat{N}_i^{vf} > 0$ (Conditions C.2 and C.5). The above inequality further leads to the following formula:

$$\sum_{j:(m\,j)\in W} \hat{Q}_{mj}^f > \sum_{j:(m\,j)\in W} \hat{Q}_{mj}^f \widetilde{\phi}_m^f = \sum_{j\in J} \widetilde{T}_{jm}^{vf} = \sum_{j\in J}\sum_{i:(i\,j)\in W} (\widehat{Pr}_{i/j} \quad \hat{Q}_{ij}^f) \geq \underline{Pr}_{i/j} \quad \frac{N^f}{2\overline{h} + \overline{w}_i^p + \overline{w}_i^{vf}} \qquad \forall i \in I. \tag{37}$$

where the first inequality stands because $\widetilde{\phi}_m^f < 1$ and second '=' results from Eq. (16b). Recall that ξ serves as a common lower bound for $N_i^{vf} \ \forall i \in I$ that satisfies $\sum_{j:(i\,j)\in W} Q_{ij}^f(N_i^{vf} \ N_i^{vc}) = \underline{Pr}_{i/j} \ \frac{N^f}{2\overline{h}+\overline{w}_i^p+\overline{w}_i^{vf}}$ for any given $N_i^{vc} \in [0 \ N^c]$ (see Lemma 2). Therefore, if (37) is satisfied, we must have $\hat{N}_m^{vf} > \xi$. However, this contradicts the assumption $N_m^{vf*} = \xi$ because $\hat{N}_m^{vf} = N_m^{vf*}$ holds at the fixed point for m. Therefore, at the fixed point, $N_i^{vf*}(\zeta^f) = \xi$ is not obtainable and $\delta_i^{f*}(\zeta^f) = 0$ and $\phi_i^{f*}(\zeta^f) = 1$ must hold for any zone $i \in I$. MNE condition (14b) and Eqs. (6d) and (6g) are satisfied.

With the updating rules $\zeta = g(\boldsymbol{N}^{vc} \ \boldsymbol{N}^{vf})$, the market status ζ is self-fulling at the fixed point because (a) $N_i^{vk*}(\zeta^k) = \hat{N}_i^{vk}$ $\forall i \in I \ k \in \{f\ c\}$ hold at the fixed point; (b) ζ^k is uniquely determined via Eqs. (10), (11), and (12) for given $(\hat{\boldsymbol{N}}_{\boldsymbol{i}}^{\boldsymbol{vc}} \ \hat{\boldsymbol{N}}_{\boldsymbol{i}}^{\boldsymbol{vf}}) \in \Omega$. Therefore, MNE condition (14c) is satisfied at the fixed point. □

B.3. Existence of multiple equilibria

We use numerical examples to show that multiple equilibria may exist for the MNE model, mainly due to the nonlinearity and nonconvexity of constraints. Using the parameters stated in Section 6, Fig. 14 presents the convergence patterns in the platform's revenue based on the best responses of freelancers and the platform. Two curves in Fig. 14 differ in their initial values of the number of idle drivers $\boldsymbol{N}^{vk}$. We observe that the calculated equilibria yield different revenue for the platform.

These two types of equilibria are also observed in other instances used in this study. Therefore, we conclude that MNE is generally not unique. To explore the potential of dual sourcing at different solutions, we run the proposed algorithm multiple times using

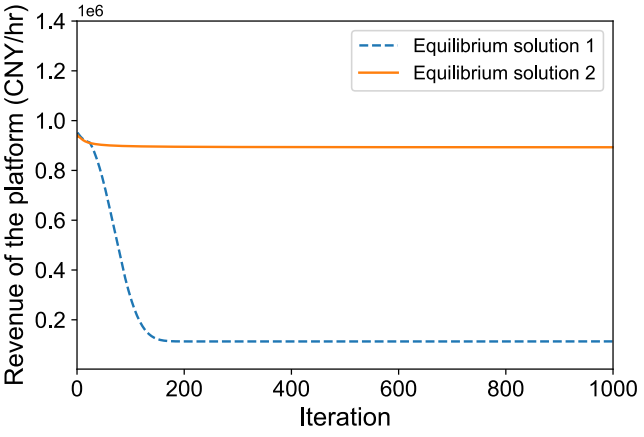

Fig. 14. The existence of multiple equilibria (20 contractors).

different starting points for $\boldsymbol{N}^{vk}$. Each starting point may display different spatial distributions of idle drivers. The equilibrium yielding the highest revenue for the platform is used as the final solution.

Appendix C. Regularity conditions and parametric setting

For notation clarification, let $x_i = (N_i^{vc} + N_i^{vf})$ denote the total number of idle drivers at each origin zone $i \in I$. Given $\boldsymbol{x} = \{x_i\}_{i \in I}$, customers' trip demand function (17) and pickup time function (18) can be restated as follows,

$$Q_{ij}(x_i) = Q_{ij}^0 \quad f(f_w(x_i)) = Q_{ij}^0 \quad \exp\left(\beta \quad (F_{ij} + \beta_w f_w(x_i))\right) - \epsilon_{ij} \qquad \forall (i \ j) \in W \tag{38a}$$

$$w_i^p(x_i) = f_w(x_i) = \frac{\eta_i}{(x_i + \epsilon_1)^\rho} \qquad \forall i \in I. \tag{38b}$$

Their derivatives regarding x_i are listed below,

$$\frac{dQ_{ij}}{dx_i} = Q_{ij}^0 \beta \beta_w \quad \exp\left(\beta \quad (F_{ij} + \beta_w f_w(x_i))\right) \quad \frac{dw_i^p}{dx_i} \qquad \forall (i \ j) \in W \tag{39a}$$

$$\frac{dw_i^p}{dx_i} = -\frac{\rho \eta_i}{(x_i + \epsilon_1)^{\rho+1}} = -\frac{\rho}{(x_i + \epsilon_1)} \quad w_i^p \qquad \forall i \in I \tag{39b}$$

$$\frac{d^2 Q_{ij}}{dx_i^2} = Q_{ij} \frac{\beta \beta_w \rho \eta_i}{(x_i + \epsilon_1)^{\rho+2}} \quad \left(\rho + 1 + \frac{\beta \beta_w \rho \eta_i}{(x_i + \epsilon_1)^\rho}\right) \qquad \forall (I \ j) \in W. \tag{39c}$$

Eqs. (38a) and (38b) define two twice-differentiable functions regarding x_i for given $\rho > 0$, which satisfies Condition C.1. Condition C.1 and C.2 require that the values of $\frac{dQ_{ij}}{dx_i}$ and pickup time w_i^p have upper limits over domain $x_i \geq 0$, which can be satisfied by setting a positive lower limit for ϵ_1 given $\eta_i > 0$ and $\rho > 0$ according to Eqs. (38b), (39a), and (39b).

Condition C.3 indicates that the number of served trips at zone i is positive when $x_i > 0$ and no trips from zone i would be served when $x_i = 0$. Section 6 mentioned that setting $\epsilon_{ij} = Q_{ij}^0 \quad \exp\left(\beta \quad (F_{ij} + \beta_w \overline{w_i^p})\right)$ will yield $\lim_{x_i \to 0} Q_{ij}(x_i) = 0$ for any OD pair $(i \ j) \in W$. With an additional definition of $\lim 0/0 = 0$, the number of trips served by type-k drivers satisfies $\lim_{x_i \to 0} Q_{ij}^k(x_i) = 0$, $\forall (i \ j) \in W$. By setting $\epsilon_1 \geq 0$, Eq. (38a) defines a continuous and increasing function on x, which ensures that $Q_{ij} > 0$ for given $x_i > 0$. Therefore, Condition C.3 can be satisfied by a parametric setting $\epsilon_{ij} = Q_{ij}^0 \quad \exp\left(\beta \quad (F_{ij} + \beta_w \overline{w_i^p})\right)$, and $\epsilon_1 \geq 0$.

Condition C.4 suggests that $f(f_w(x_i))$ is strictly concave regarding x_i, or equivalently $\frac{d^2 Q_{ij}}{dx_i^2} < 0 \ \forall (i \ j) \in W$. According to Eq. (39c), for any given $\rho \eta_i > 0$ and $\beta \beta_w < 0$, Condition C.4 holds if $-\beta \beta_w / (x_i + \epsilon_1)^\rho < \rho + 1$ where the term on the right-hand side attains its maximum at $x_i = 0$. Therefore, Condition C.4 is satisfied by setting $\epsilon_1 \geq (-\beta \beta_w \rho \eta_i / (\rho + 1))^{1/\rho}$.

Condition C.5 requires the term $x_i / f(f_w(x_i))$ to be upper-bounded so that drivers' average waiting time, which is calculated by $\frac{x_i}{\sum_{j:(i,j) \in W} Q_{ij}}$, has an upper limit. Since $x_i \leq N^c + N^f$ and $f(f_w(x_i))$ defines a continuous increasing function with x_i, showing that $x_i / f(f_w(x_i))$ has a upper limit is equivalent to showing that $\lim_{x_i \to 0} x_i / f(f_w(x_i))$ exists. Applying L'Hospital's Rule gives:

$$\lim_{x_i \to 0} \frac{x_i}{f(f_w(x_i))} = \lim_{x_i \to 0} \frac{Q_{ij}^0}{\frac{dQ_{ij}}{dx_i}} = Q_{ij}^0 \quad \frac{(\epsilon_1)^{\rho+1}}{-\epsilon_{ij} \beta \beta_w \rho \eta_i} \qquad \forall i \in I.$$

The above formula indicates that Condition C.5 holds over the domain $x \in (0 \ \ N^c + N^f)$ by setting a lower limit for ϵ_{ij} and an upper bound for ϵ_1.

Summarizing the above analysis, Condition C.1–C.5 holds with a parametric setting $\epsilon_1 \in [-\beta\beta_w\rho\eta_i/(\rho+1))^{1/\rho}\ \infty)$, and $\epsilon_{ij} = Q^0_{ij}\ \exp\left(\beta\ \ (F_{ij}+\beta_w\overline{w_i^p})\right)\ \forall(i\ j)\in W$. For the numerical experiments introduced in Section 7, we set $\epsilon_1 = 0.8$.

Appendix D. Matching module with driver priority

In this appendix, we derive the mathematical expressions for the matching probability and pickup time at an arbitrary origin zone $i \in I$ under the context of matching priority.

Matching probability. For a given zone $i \in I$, let A_i be its area and $\lambda_i^k (= N_i^{vk}/A_i)$ be the average density of type-k drivers idling in the zone. Denote $\ _i^k(n\ r)$ as the probability that a circular area of radius r contains exactly n idle type-k drivers. By assuming that idle drivers appear randomly in space following a Poisson Point Process, $\ _i^k(n\ r)$ can be expressed as

$$\ _i^k(n\ r) = \frac{(\lambda_i^k \pi r^2)^n}{n}\ \ e^{-\lambda_i^k \pi r^2} \quad \forall k \in \{f\ \ c\}. \tag{40}$$

Suppose freelancers (contractors) are discriminated (prioritized) with a distance adjustment ratio of α_i. Following the priority mechanism expounded in Section 8, the probability of a customer being matched with an idle contractor who is r away is

$$P_i^c(r) = \ _i^f\left(0\ \frac{r}{\alpha_i}\right)\ \left(\ _i^c(1\ r+\mathrm{d}r) - \ _i^c(0\ r)\right).$$

where $\mathrm{d}r$ represents an infinitesimal distance. Then, applying Eq. (40) and omitting the higher-order terms on $\mathrm{d}r$ yields

$$P_i^c(r) = 2\lambda_i^c \pi r\ \ e^{-\pi r^2\ (\lambda_i^c+\lambda_i^f/\alpha_i^2)}\mathrm{d}r. \tag{41}$$

Then, integrating the above item over r from 0 to $+\infty$ obtains the unconditional probability P_i^c of a customer matched with an idle contractor as follows,

$$P_i^{\ c} = \int_0^\infty 2\lambda_i^c \pi r\ \ e^{-\pi r^2\ (\lambda_i^c+\lambda_i^f/\alpha_i^2)}\mathrm{d}r = \frac{\alpha_i^2 N_i^{vc}}{\alpha_i^2 N_i^{vc} + N_i^{vf}}.$$

The complement to 1 of P_i^c gives the customer's probability of matching with a freelancer,

$$P_i^{\ f} = 1 - P_i^{\ c} = \frac{N_i^{vf}}{\alpha_i^2 N_i^{vc} + N_i^{vf}}.$$

Pickup time. Suppose a customer in zone i gets matched to an idle contractor. Using Eq. (41), the unconditional expected pickup time w_i^{pc} for the contractor could be derived as follows (Zha et al., 2018b),

$$w_i^{pc} = \frac{1}{v_i P_i^c}\ \ \int_0^\infty 2\lambda_i^c \pi r^2\ \ e^{-\pi r^2\ (\lambda_i^c+\lambda_i^f/\alpha_i^2)}\mathrm{d}r = \frac{\alpha_i\sqrt{A_i}}{2v_i\sqrt{\alpha_i^2 N_i^{vc} + N_i^{vf}}}$$

where v_i is the vehicle's average travel speed in zone i. Similarly, for freelancers, the contingent expected pickup time w_i^{pf} is

$$w_i^{pf} = \frac{\sqrt{A_i}}{2v_i\sqrt{\alpha_i^2 N_i^{vc} + N_i^{vf}}}.$$

Thus, by introducing parameter $\eta_i = \frac{\sqrt{A_i}}{2v_i}$, we write drivers' expected pickup time w_i^{pk} as

$$w_i^{pf} = \eta_i/\sqrt{\alpha_i^2\ \ N_i^{vc} + N_i^{vf}} \qquad w_i^{pc} = \alpha_i w_i^{pf}. \tag{42}$$

Meanwhile, from customers' view, the expected pickup time w_i^p is

$$w_i^p = P_i^c\ \ w_i^{pc} + P_i^f\ \ w_i^{pf}.$$

Appendix E. Discussion on dual sourcing under dynamic market setting

To account for market temporal variations, one can equally divide the planning horizon into a set of discrete periods $\mathcal{H} = \{1\ 2\ \dots\ t\ \dots\}$. At each period t, the market state is characterized as a tuple $S^{(t)} = \{\boldsymbol{N}^{vk(t)}\ \boldsymbol{Q}^{k(t)}\ \boldsymbol{T}^{vk(t)}\ \{w_i^{vk(t)}\}_{i\in I}\ \{w_i^{p(t)}\}_{i\in I}\}$ where $\boldsymbol{Q}^{k(t)}$ and $\boldsymbol{T}^{vk(t)}$ represent the spatial distribution of type-k drivers who are delivering customers to their destinations and who are repositioning toward their target zones by time t, respectively. $w_i^{vk(t)}$ and $w_i^{p(t)}$ denote drivers' idle time and the pick-up time for customers at the start of period t. The market state over both temporal and spatial dimensions can be represented as $\mathcal{S} = \{S^{(t)}\}_t$.

Similar to the static model, the platform determines the flow of contractors after dropping off customers while freelancers strategically choose target zones. At the start of period t, we characterize the platform's repositioning policy $\mathcal{R}^t$ by the fraction of contractors who cruise from each destination zone toward their designated zones:

$$\mathcal{R}^t = \left\{ \Lambda_{ji}^{c(t)} \in [0\ \ 1] \middle| T_{ji}^{c(t)} = \Lambda_{ji}^{c(t)} \sum_{\tilde{t}\in\mathcal{H}\ \ o:(o\ j)\in W} (\tilde{t} + w_o^{p(\tilde{t})} + h_{oj} = t)\ \ Q_{oj}^{c(\tilde{t})} \right\} \quad \forall t \in \mathcal{H}$$

where (x) stands for an indicator function whose value is 1 if x is true and 0 otherwise; $Q_{ij}^{c(\bar{t})}$ is the number of trips between OD pair $(i\ j)$ that are served by contractors at t. For freelancers within the destination zone j, we characterize their repositioning strategies by their probability of choosing each origin zone $\{Pr_{i/j}^{(t)}\}$. Applying Eq. (3) leads to the following formula:

$$Pr_{i/j}^{(t)} = \frac{\exp(\theta U_{ji}^{(t)})}{\sum_{m\in I}\exp(\theta U_{jm}^{(t)})} \quad \forall i \in I\ \ j \in J\ \ t \in \mathcal{H}$$

where $U_{ji}^{(t)}$ represents freelancers' expected utility for cruising from j to i at period t.

The following fixed point problem can be employed to capture the intricate interaction between market demand and repositioning decisions:

$$\begin{aligned}
&\mathcal{S} = F_1(\{\mathcal{R}^{(t)}\}_t\ \ \{Pr_{i/j}^{(t)}\}_{t\,j\,i});\\
&\{\mathcal{R}^{(t)}\}_t = F_2(\mathcal{S})\\
&\{Pr_{i/j}^{(t)}\ \ U_{ji}^{(t)}\}_{t\,j\,i} = F_3(\mathcal{S})
\end{aligned}$$

where function $F_1(\,)$ accounts for system dynamics given the platform's and freelancers' repositioning decisions; functions $F_2(\,)$ and $F_3(\,)$ prescribe the platform and freelancers' best responses. In a dynamic market setting, one research direction would be to characterize the market state variation pattern $F_1(\,)$. This is nontrivial because $F_1(\,)$ accommodates various endogenous relations between market demand and supply.

Another research direction involves investigating "far-sighted" repositioning behaviors when modeling drivers' best response functions $F_2(\,)$ and $F_3(\,)$. For example, for a freelancer at zone j, her utility of choosing origin zone i can be expressed as follows:

$$\begin{aligned}
U_{ji}^{(t)}(\mathcal{S}) =\ & -\gamma_1\ \ h_{ji} - \gamma_2\ \ w_i^{vf(t+h_{ji})}(\mathcal{S})\\
&+ \frac{1}{\sum_{d:(i\,d)\in W} Q_{id}^{k(\bar{t}_1)}}\ \ \left[\sum_{d:(i\,d)\in W} Q_{id}^{k(\bar{t}_1)}\ \ \left(E_{id} - \gamma_1\ \ h_{id} + \gamma_3\ \ \overline{U}_d^{\bar{t}_2}(\mathcal{S})\right)\right]\\
&\forall j \in J\ \ i \in I\ \ t \in \mathcal{H}
\end{aligned} \tag{43}$$

where $\bar{t}_1 = t + h_{ji} + w_i^{vf(t+h_{ji})}$ and $\bar{t}_2 = \bar{t}_1 + h_{id}$; $\overline{U}_d^{\bar{t}_2}$ denotes the drivers' expected future utility after delivering a customer from origin i to destination d. It can be calculated by $\overline{U}_j^{t}(\mathcal{S}) = \sum_{i\in I} Pr_{i/j}^{(t)}\ \ U_{ji}^{(t)}(\mathcal{S}) \quad \forall j \in J\ \ t \in \mathcal{H}$; and $\boldsymbol{\gamma}$ denotes a set of coefficients for different utility factors. On the right-hand side of Eq. (43), the first line describes drivers' total cost before getting matched in zone i. The second line represents drivers' expected revenue and costs for serving customers at zone i. In particular, $\overline{U}_d^{\bar{t}_2}$ is incorporated to account for freelancers' far-sighted repositioning behaviors. The coefficient γ_3 is a discount factor and would replicate myopic decisions if it equals 0. By defining freelancers' utility as Eq. (43), their far-sighted behavior influences their best response to market states. The impact of such behaviors on market states and players merits further investigation.

References

Afeche, P., Liu, Z., Maglaras, C., 2023. Ride-hailing networks with strategic drivers: The impact of platform control capabilities on performance. Manuf. Serv. Oper. Manage. 25 (5), 1890–1908.

Ausubel, L.M., Deneckere, R.J., 1993. A generalized theorem of the maximum. Econom. Theory 3 (1), 99–107.

Banerjee, S., Freund, D., Lykouris, T., 2017. Pricing and optimization in shared vehicle systems: An approximation framework. In: Proceedings of the 2017 ACM Conference on Economics and Computation. pp. 517–517.

Beojone, C.V., Geroliminis, N., 2023. Relocation incentives for ride-sourcing drivers with path-oriented revenue forecasting based on a Markov chain model. Transp. Res. C 157, 104375.

Besbes, O., Castro, F., Lobel, I., 2021. Surge pricing and its spatial supply response. Manage. Sci. 67 (3), 1350–1367.

Bimpikis, K., Candogan, O., Saban, D., 2019. Spatial pricing in ride-sharing networks. Oper. Res. 67 (3), 744–769.

Braverman, A., Dai, J.G., Liu, X., Ying, L., 2019. Empty-car routing in ridesharing systems. Oper. Res. 67 (5), 1437–1452.

Buchholz, N., 2022. Spatial equilibrium, search frictions, and dynamic efficiency in the taxi industry. Rev. Econom. Stud. 89 (2), 556–591.

Cachon, G.P., Daniels, K.M., Lobel, R., 2017. The role of surge pricing on a service platform with self-scheduling capacity. Manuf. Serv. Oper. Manag. 19 (3), 368–384.

Castillo, J.C., Knoepfle, D., Weyl, G., 2017. Surge pricing solves the wild goose chase. In: Proceedings of the 2017 ACM Conference on Economics and Computation. pp. 241–242.

Castillo, E., Menéndez, J.M., Jiménez, P., Rivas, A., 2008. Closed form expressions for choice probabilities in the Weibull case. Transp. Res. B 42 (4), 373–380.

Chen, L., Mislove, A., Wilson, C., 2015. Peeking beneath the hood of uber. In: Proceedings of the 2015 Internet Measurement Conference. pp. 495–508.

Chen, X.M., Zheng, H., Ke, J., Yang, H., 2020. Dynamic optimization strategies for on-demand ride services platform: Surge pricing, commission rate, and incentives. Transp. Res. B 138, 23–45.

Daganzo, C.F., 1978. An approximate analytic model of many-to-many demand responsive transportation systems. Transp. Res. 12 (5), 325–333.

Davidson, M., 1996. Stability of the extreme point set of a polyhedron. J. Optim. Theory Appl. 90 (2), 357–380.

Dong, J., Ibrahim, R., 2020. Managing supply in the on-demand economy: Flexible workers, full-time employees, or both? Oper. Res. 68 (4), 1238–1264.

Dong, T., Xu, Z., Luo, Q., Yin, Y., Wang, J., Ye, J., 2021. Optimal contract design for ride-sourcing services under dual sourcing. Transp. Res. B 146, 289–313.

Garg, N., Nazerzadeh, H., 2021. Driver surge pricing. Manage. Sci. 68 (5), 3219–3235.

Granas, A., Dugundji, J., 2003. Fixed Point Theory. Vol. 14, Springer.

Guda, H., Subramanian, U., 2019. Your Uber is arriving: Managing on-demand workers through surge pricing, forecast communication, and worker incentives. Manage. Sci. 65 (5), 1995–2014.

Guide, A.H., 2006. Infinite Dimensional Analysis. Springer.

Guo, X., Caros, N.S., Zhao, J., 2021. Robust matching-integrated vehicle rebalancing in ride-hailing system with uncertain demand. Transp. Res. B 150, 161–189.
Hall, J., Kendrick, C., Nosko, C., 2015. The Effects of Uber's Surge Pricing: a Case Study. The University of Chicago, Chicago, IL.
Harker, P.T., 1988. Multiple equilibrium behaviors on networks. Transp. Sci. 22 (1), 39–46.
He, F., Wang, X., Lin, X., Tang, X., 2018. Pricing and penalty/compensation strategies of a taxi-hailing platform. Transp. Res. C 86, 263–279.
Iglesias, R., Rossi, F., Zhang, R., Pavone, M., 2019. A BCMP network approach to modeling and controlling autonomous mobility-on-demand systems. Int. J. Robot. Res. 38 (2–3), 357–374.
Jiao, Y., Tang, X., Qin, Z.T., Li, S., Zhang, F., Zhu, H., Ye, J., 2021. Real-world ride-hailing vehicle repositioning using deep reinforcement learning. Transp. Res. 130, 103289.
Lei, Z., Qian, X., Ukkusuri, S.V., 2020. Efficient proactive vehicle relocation for on-demand mobility service with recurrent neural networks. Transp. Res. C 117, 102678.
Li, S., Luo, Q., Hampshire, R.C., 2021. Optimizing large on-demand transportation systems through stochastic conic programming. European J. Oper. Res. 295 (2), 427–442.
Liu, H.X., He, X., He, B., 2009. Method of successive weighted averages (MSWA) and self-regulated averaging schemes for solving stochastic user equilibrium problem. Netw. Spat. Econ. 9, 485–503.
Liu, Y., Samaranayake, S., 2020. Proactive rebalancing and speed-up techniques for on-demand high capacity ridesourcing services. IEEE Trans. Intell. Transp. Syst. 23 (2), 819–826.
Lu, A., Frazier, P., Kislev, O., 2018. Surge pricing moves uber's driver partners. Available at SSRN 3180246.
Luenberger, D.G., Ye, Y., et al., 1984. Linear and Nonlinear Programming. Vol. 2, Springer.
Ma, J., Xu, M., Meng, Q., Cheng, L., 2020. Ridesharing user equilibrium problem under OD-based surge pricing strategy. Transp. Res. B 134, 1–24.
Narayanan, S., Chaniotakis, E., Antoniou, C., 2020. Shared autonomous vehicle services: A comprehensive review. Transp. Res. C 111, 255–293.
Özkan, E., Ward, A.R., 2020. Dynamic matching for real-time ride sharing. Stoch. Syst. 10 (1), 29–70.
Robinson, S.M., 1977. A characterization of stability in linear programming. Oper. Res. 25 (3), 435–447.
Solodov, M.V., et al., 2010. Constraint qualifications. In: Wiley Encyclopedia of Operations Research and Management Science. Wiley, New York.
Still, G., 2018. Lectures on parametric optimization: An introduction. Optim. Online.
Taylor, T.A., 2018. On-demand service platforms. Manuf. Serv. Oper. Manag. 20 (4), 704–720.
Tian, G., Zhou, J., 1992. The maximum theorem and the existence of Nash equilibrium of (generalized) games without lower semicontinuities. J. Math. Anal. Appl. 166 (2), 351–364.
Tripathy, M., Bai, J., Heese, H.S., 2022. Driver collusion in ride-hailing platforms. Decis. Sci. 54 (4), 434–446.
Urata, J., Xu, Z., Ke, J., Yin, Y., Wu, G., Yang, H., Ye, J., 2021. Learning ride-sourcing drivers' customer-searching behavior: A dynamic discrete choice approach. Transp. Res. C 130, 103293.
Wang, H., Yang, H., 2019. Ridesourcing systems: A framework and review. Transp. Res. B 129, 122–155.
Wei, Q., Pedarsani, R., Coogan, S., 2020. Mixed autonomy in ride-sharing networks. IEEE Trans. Control Netw. Syst. 7 (4), 1940–1950.
Wei, Q., Rodriguez, J.A., Pedarsani, R., Coogan, S., 2019. Ride-sharing networks with mixed autonomy. In: 2019 American Control Conference (ACC). IEEE, pp. 3303–3308.
Wen, J., Zhao, J., Jaillet, P., 2017. Rebalancing shared mobility-on-demand systems: A reinforcement learning approach. In: 2017 IEEE 20th International Conference on Intelligent Transportation Systems (ITSC). IEEE, pp. 220–225.
Wong, K., Wong, S., Yang, H., 1999. Calibration and validation of network equilibrium taxi model for Hong Kong. In: Transportation Science and Technology Into the Next Millenium: Proceedings of the Fourth Conference of the Hong Kong Society for Transportation Studies, Hong Kong, HKUST, Hong Kong.
Wong, K.-I., Wong, S.C., Yang, H., 2001. Modeling urban taxi services in congested road networks with elastic demand. Transp. Res. B 35 (9), 819–842.
Wong, S., Yang, H., 1998. Network model of urban taxi services: Improved algorithm. Transp. Res. Rec. 1623 (1), 27–30.
Xu, Z., Chen, Z., Yin, Y., Ye, J., 2021a. Equilibrium analysis of urban traffic networks with ride-sourcing services. Transp. Sci. 55 (6), 1260–1279.
Xu, Z., Yin, Y., Chao, X., Zhu, H., Ye, J., 2021b. A generalized fluid model of ride-hailing systems. Transp. Res. B 150, 587–605.
Xu, Z., Yin, Y., Ye, J., 2020. On the supply curve of ride-hailing systems. Transp. Res. B 132, 29–43.
Yang, H., Fung, C., Wong, K.I., Wong, S.C., 2010a. Nonlinear pricing of taxi services. Transp. Res. A 44 (5), 337–348.
Yang, H., Leung, C.W., Wong, S.C., Bell, M.G., 2010b. Equilibria of bilateral taxi–customer searching and meeting on networks. Transp. Res. B 44 (8–9), 1067–1083.
Yang, Y., Ramezani, M., 2022. A learning method for real-time repositioning in E-hailing services. IEEE Trans. Intell. Transp. Syst. 24 (2), 1644–1654.
Yang, K., Tsao, M.W., Xu, X., Pavone, M., 2020. Planning and operations of mixed fleets in mobility-on-demand systems. arXiv preprint arXiv:2008.08131.
Yang, H., Wong, S.C., 1998. A network model of urban taxi services. Transp. Res. B 32 (4), 235–246.
Zardini, G., Lanzetti, N., Pavone, M., Frazzoli, E., 2022. Analysis and control of autonomous mobility-on-demand systems. Annu. Rev. Control, Robot., Auton. Syst. 5, 633–658.
Zha, L., Yin, Y., Du, Y., 2018a. Surge pricing and labor supply in the ride-sourcing market. Transp. Res. B 117, 708–722.
Zha, L., Yin, Y., Xu, Z., 2018b. Geometric matching and spatial pricing in ride-sourcing markets. Transp. Res. C 92, 58–75.
Zhang, K., Mittal, A., Djavadian, S., Twumasi-Boakye, R., Nie, Y.M., 2023. Ride-hail vehicle routing (RIVER) as a congestion game. Transp. Res. B 177, 102819.
Zuniga-Garcia, N., Tec, M., Scott, J.G., Ruiz-Juri, N., Machemehl, R.B., 2020. Evaluation of ride-sourcing search frictions and driver productivity: A spatial denoising approach. Transp. Res. C 110, 346–367.